


5-2018

GIS Modeling of the Prominent Geohazards in Arkansas

Kyle Walker Rowden
University of Arkansas, Fayetteville

Follow this and additional works at: <http://scholarworks.uark.edu/etd>

 Part of the [Geographic Information Sciences Commons](#), [Geology Commons](#), and the [Meteorology Commons](#)

Recommended Citation

Rowden, Kyle Walker, "GIS Modeling of the Prominent Geohazards in Arkansas" (2018). *Theses and Dissertations*. 2803.
<http://scholarworks.uark.edu/etd/2803>

This Thesis is brought to you for free and open access by ScholarWorks@UARK. It has been accepted for inclusion in Theses and Dissertations by an authorized administrator of ScholarWorks@UARK. For more information, please contact scholar@uark.edu, ccmiddle@uark.edu.

GIS Modeling of the Prominent Geohazards in Arkansas

A thesis submitted in partial fulfillment
of the requirements for the degree of
Master of Science in Geology

by

Kyle Walker Rowden
Arkansas Tech University
Bachelor of Science in Geology, 2016

May 2018
University of Arkansas

This thesis is approved for recommendation to the Graduate Council.

Mohamed H. Aly, Ph.D.
Thesis Director

Gregory Dumond, Ph.D.
Committee Member

Jason A. Patton, Ph.D.
Committee Member

ABSTRACT

The State of Arkansas is prone to numerous geohazards. This thesis is a twofold study of prominent geohazards in Arkansas: the first fold includes a novel triggerless approach for mass wasting susceptibility modeling applied to the Boston Mountains in NW Arkansas, and the second fold is a GIS-based regression modeling of the extreme weather patterns at the state level. Each study fold is presented in this thesis as a separate chapter embracing a published peer-reviewed paper. In the first paper, I have used the analytical hierarchy process to assign preliminary statistical weights to the most cogent variables influencing mass wasting in the central Boston Mountains. These most significant variables are then incorporated in Fuzzy modeling of mass wasting susceptibility within the 1200 km² study area. For comparison and accuracy assessment, a second model has been established using a conventional weighted overlay (WO) approach. Results indicate that the developed novel approach is superior, with approximately 83% accuracy, to the traditional WO approach that has a marginal success of about 28% accuracy. Road related mass wasting events recorded by the Arkansas Department of Transportation have been used to validate both models. In the second paper, I have conducted a systematically gridded analysis of severe weather events, including tornadoes, derechos, and hail, during 1955-2015. The study examines and statistically determines the most significant explanatory variables contributing to the spatial patterns of severe weather events between 1955 and 2015, consequently it identifies severity indices for the entire state. These weather-related hazards and their associated risk will always abide; therefore, the best defense is employ geospatial technologies to plan for hazard mitigation. The mass wasting model developed in this study contributes pivotal information for identifying zones of high risk along roadways in NW Arkansas, which definitely can be adapted to avoid disastrous road failures. In addition, the weather-related severity indices determined at the

state level can profoundly benefit state and federal agencies focused on increasing the availability of public and private storm shelters in previously under-represented zones of high risk. This undoubtedly will save lives from unavoidable catastrophic events across the entire state.

© 2018 by Kyle Walker Rowden
All Rights Reserved

ACKNOWLEDGEMENTS

Thank you, Sarah Pennington, my fiancé, for standing by me through this entire process. She has somehow found the strength and patience to stay with me through my personal triumphs and all the rock bottom lows we endured while I pursued my higher education.

I must extend an infinite amount of thanks and gratitude to my thesis director, Dr. Mohamed Aly, for accepting me as one of his students when I lacked nearly any meritable experience in conducting intensive scientific research in his field. Dr. Aly challenged me more than I have ever been challenged in my life. He kept constant pressure on me and like a medic covering a wound, but he continuously yielded with patience to step me through this process. He has opened my eyes to the standards of the science community and unrelentingly inspired me to hold true to these highest standards in science. He has taught me so much about geology, remote sensing, GIS, conducting proper research, integrity, perseverance, and he always set a bar for me just beyond what I could grasp; making me jump and pushing me further and further along. I am indebted to his kindness and tutelage.

I would like to both of my ancillary committee members. Thank Dr. Jason Patton for getting me this far in my academic career and being a sound voice of pragmatic reason in a world of high paced chaotic energy to get results now without stopping to take a breath and thinking through a problem. For instilling the virtue of throwing away as many iterations of project necessary to deliver something as close to perfection as I'm capable. I extend many thanks to Dr. Greg Dumond for being a part of this elite cadre selected to serve on my thesis committee. I value his time and the unique knowledge he brings to this thesis committee.

To family and friends, I love you all and I thank you so much for being here still. Returning to school to earn a Bachelor's in my late twenties and then immediately pursuing this master's degree placed much of my life on hold. I chose to make many sacrifices, just as my loved ones and close friends had to make sacrifices in my absence. I missed birthdays, weddings, and funerals because I put school before family. I hope you will be able to forgive me. This process has been far from easy and I have questioned this decision everyday but all that is behind me and I can now stand here at the gate to my future and be released.

Last but not least, I must credit all my data sources and funding opportunities that relates to this research. This research project was fully funded by a NASA EPSCoR RID grant #24203116UAF awarded to Dr. Aly. Computers, software, and lab equipment used exclusively for this research were made available thanks to the Center for Advanced Spatial Technologies and the InSAR Research Laboratory at the University of Arkansas. I am much obliged to John Wilson, Panagiotis Giannakis and Brandon Flessner for technical troubleshooting. Data collection came from numerous sources: Arkansas Geological Survey, Arkansas Department of Transportation, Arkansas Spatial and Data Infrastructure, Environmental Systems Research Institution, National Oceanic and Atmospheric Agency, Natural Resources Commission Service, Storm Prediction Center Severe Weather GIS, United States Department of Agriculture, United States Geological Survey.

TABLE OF CONTENTS

CHAPTER 1	1
INTRODUCTION	1
MASS WASTING SUSCEPTIBILITY	2
SEVERE WEATHER EVENTS	3
RESEARCH CONTRIBUTIONS	5
CHAPTER 2	7
ABSTRACT	7
INTRODUCTION	8
MASS WASTING INVENTORY FOR NW ARKANSAS	11
DATASETS	14
METHODS	17
RESULTS AND DISCUSSIONS	30
CONCLUSIONS	35
ACKNOWLEDGEMENTS	37
REFERENCES	38
CHAPTER 3	42
GIS-BASED REGRESSION MODELING OF THE EXTREME WEATHER PATTERNS IN ARKANSAS, USA	42
ABSTRACT	42
INTRODUCTION	43
METHODOLOGY	51
RESULTS AND DISCUSSION	57
CONCLUSIONS	69
DECLARATIONS	71
ACKNOWLEDGEMENTS	71
REFERENCES	72
CHAPTER 4	76
CONCLUSION	76
REFERENCES	80

LIST OF PUBLISHED PAPERS

1. Rowden KW, Aly MH (2018) A novel triggerless approach for mass wasting susceptibility modeling applied to the Boston Mountains of Arkansas, USA, *Natural Hazards*, pp 1–21, doi:10.1007/s11069-018-3201-7
2. Rowden KW, Aly MH (2018) GIS-based regression modeling of the extreme weather patterns in Arkansas, USA, *Geoenvironmental Disasters*, pp 1-15, doi:10.1186/s40677-018-0098-0

CHAPTER 1

INTRODUCTION

Arkansas has not had the pleasure of vast scientific exploration like other more populous states that reap the benefits of having numerous research institutions with large pools of scientific funding and plethora of state institutions examining all the scientific minutia associated within their state's boundary. On one side of the coin this is extremely problematic and frustrating as a researcher trying to collate a body of previously published peer-reviewed research for a quality literature review. Much of the material available on specific problems, especially those related to geohazards, only exists in sparse white papers from the Arkansas Geological Survey (AGS) and tidbits from United States Geological Survey (USGS), the Federal Emergency Management Agency (FEMA), the National Weather Service (NWS) and a handful of graduate publications. With respect to mass wasting/mass movement and severe weather these few publications range from the 1950's through present and mostly serve only as historical recording of events and magnitudes with quality but superficial interpretations of underlying causality. For a researcher choosing to focus on geohazards in Arkansas, outside of earthquakes, minimal research has been done and any new work will have to be conducted nearly from scratch. The other side of the coin is a vast field of opportunity in nearly all directions for scientific research related to Arkansas.

Many types of geospatial software exist but possibly no geospatial software is more pervasive than ArcGIS. The near endless and ever improving capabilities of the spatial and geostatistical tools developed by the Environmental Systems Research Institute (ESRI) offer a profusion of opportunities to model and analyze the complexities inherent in big data sets. The proliferation of ArcGIS in academia as well as many private and public research institutions allows for provenance to be easily preserved and analytical outputs scrutinized and reproduced for

viability of the scientific approach used in any GIS analysis using ArcGIS. For these reasons ArcGIS was selected to be exclusively used in all modeling and analysis related to this research.

MASS WASTING SUSCEPTIBILITY

Arkansas can be roughly broken into two to eight regions depending on the amount of detail considered by the defining source. For this particular research seven physiographic regions have been defined and general descriptions are: (1) the Mississippi Alluvial Plain, a lowland floodplain region of unconsolidated Quaternary sediments which extends along the entire eastern margin of the state delineating a large regional distributary system within the Gulf Coastal Plain (GCP) for the largest rivers in Arkansas as well as present and paleo floodplains for the Mississippi River (Berry 1915; Haley 1976); (2) Crowley's Ridge, a 250km long and 50-100m high ridge that extends longitudinally through the heart of the Mississippi Alluvial Plain and has been interpreted as a tectonically active high angle reverse fault block of unconsolidated Tertiary and Miocene sediments, most likely associated with the New Madrid Fault Zone and Reel Foot Rift (Guccione et al. 1986); (3) the South Central Plains, also referred to as the West Gulf Coastal Plain is a region of gentle rolling hills in the southwestern region of the (GCP) along the Texas/Louisiana borders comprised of Cretaceous carbonates and evaporites as well as Tertiary clays and lignite, and Quaternary gravels and sands (Hill 1888; Harris 1894; Dane 1929; Clardy 1979); (4) the Ouachita Mountains in the west central part of the state are heavily folded and deformed Paleozoic strata with dominant strikes running East-West (Croneis 1930; Sutherland and Manger 1979); (5) the Arkansas River Valley, which consists of gently to moderately deformed Pennsylvanian strata and is commonly associated with the Arkansas River and I-40 corridor stretching from the Oklahoma state line to Little Rock (Croneis 1930; Haley 1976; Cohoon 2013); (6) the Boston Mountain Plateau which is slightly to moderately faulted and gently deformed region of uplifted Late-

Paleozoic strata; and lastly (Sutherland and Manger 1977; Cohoon 2013) (7) the Ozark Highlands region which includes both the Salem and Ozark Plateaus which are dominantly composed of Mississippian and Ordovician carbonates promoting a vast karst network (Craig et al. 1979).

Each of these regions contains unique geology and underlying geologic structure which juxtapose the Ouachita Mountains and deeply incised mature plateaus in the western half of the state to the flat fertile agricultural bottomlands of the Arkansas Delta in the east. Mass wasting may occur where there is sufficient relief and slope instability. This being said, the vast majority of mass wasting events in Arkansas occurs in the Boston Mountains and the Ozark Highlands. Because of this natural susceptibility for frequent mass wasting events in these regions, a study area was chosen within the central Boston Mountains along the Arkansas Highway 7 due to the frequency of events and availability of quality GIS data from AGS.

Mass wasting events were compiled from an internal database collected by the Arkansas Department of Transportation (ArDOT) and through case studies conducted by AGS. A weighting process using Saaty's Analytical Hierarchy Process helped statistically quantify the significance of geologic and physiographic attributes which were then modeled using a combination of Fuzzy logic and Empirical Bayesian Kriging (EBK) to create a triggerless mass wasting susceptibility model for the 1200 km² study area. For comparison with the established model, a traditional Weighted Overlay (WO) model was developed. Results indicate that the model developed via the Fuzzy/EBK approach proved significantly more accurate at predicting mass wasting susceptibility with ~83% accuracy of predicting the observed failures versus an unanticipated marginal (~28%) accuracy using the conventional WO process that showed a heavy road bias.

SEVERE WEATHER EVENTS

Wild variability in the local weather of Arkansas is very common. One day it can be 75°F and sunny with bluebird skies and then the next day it can snow. These extremely variable temperature swings are due to Arkansas' location in the middle of the High and Low-pressure ridges. High pressure coming out of the northern United States and Canada pushes down through the Great Plains and typically collides somewhere around Arkansas with warm moist low-pressure systems coming up from the Gulf of Mexico. Prevailing westerly winds end up driving storm fronts, which nucleate during the collision of these combative pressure systems, eastward across the state. Many time these storm systems spawn severe thunderstorms capable of generating hail, high wind events called derechos, and/or tornadoes. Many lives have been lost in Arkansas due to tornadoes and derechos crossing paths with people both in their homes or out in the open away from storm shelters.

Previous studies conducted by FEMA or state agencies rarely goes beyond the scope of county analysis. In Arkansas, counties range broadly in terms of physiographic and topographic characteristics and that is not appropriate for the nature of the desired modeling of the extreme weather events. The solution applied in this research, was to fishnet the entire state in 10 x 10 km grids and then assign all the potential explanatory variables to an attribute table associated with the fishnet. Once all the datasets were standardized and associated with the fishnet, exploratory regression and Ordinary Least Squares regression were applied to develop the final model. Ultimately, a statewide severity index was created by combining all three models, which allowed a very high detailed statewide analysis of severe weather that had never been conducted before. Spatial analysis of severe weather patterns using GIS provides a means of determining major influencing variables in the equation that drive these storm patterns across the state. GIS-based

regression analysis was applied to sort the variables and pick out the most statistically robust explanatory variables to model statewide severity for each of the three types of severe weather events.

RESEARCH CONTRIBUTIONS

Research conducted in this thesis provides a wealth of information to several Arkansas state agencies such, as the Arkansas Department of Emergency Management (ADEM), the Governor's Office, ArDOT, AGS, and academic intuitions that may wish to continue the conducted research as well as federal agencies such as FEMA, NOAA, NWS, USGS, Natural Resources Commission Service NRCS, and USDA.

With respect to the mass wasting study, this research can immediately benefit ArDOT and allow it to strategize in an entirely new way to better plan how it can mitigate road failures. Currently, ArDOT is looking into soil nailing mitigation techniques by determining high risk sections of roads that have not failed and reinforcing these compromised areas before failure occurs and traffic and commerce has to be drastically altered elsewhere until the roadway is repaired. Also, AGS could easily scale the developed approach to work with much of the Boston Mountain region. Due to the nature of AGS's GIS data being generally unavailable to the public, it is really the only agency that could easily continue working on this project at a larger scale as the backbone of this research relied heavily on the detailed 15-minute surveys conducted by AGS over the past decade. There is still much of the western Boston Mountains left to survey at the detailed 15-minute quadrangle level, so a holistic model using the triggerless developed approach is still not presently feasible and, leaves the door open for applying this strategy in the future. A catalog of 400+ mass wasting events has been collated for this research and can be requested for future use. Limitations within ArDOT's data was brought to their attention and improvements have been made

on their part, to strengthen future data collection which will provide a greater depth and variability to future research examining time domains.

Contributions related to severe weather analysis conducted as part of this thesis may have the most valuable impact on the state because this research has the potential to save lives and reduce injuries associated with severe weather by providing some of the highest detailed statistical analysis conducted for the state of Arkansas. Severity prediction can reduce the feeling of complacency perturbed by previous county assessment and will hopefully educate a greater percentage of Arkansans who live in areas prone to these severe weather patterns. This detailed analysis can provide the extra incentive to influence people and communities to build more storm shelters, overall providing the state with a greater abundance of private and public safe zones. State and federal grants exist that will greatly subsidize the cost of building storm shelters but surprisingly few Arkansans even know these options are available. Neighborhoods could come together and build shelters that could prevent tragedies like the April 2014 Mayflower Tornado, which tore through the Parkwood Meadows subdivision and ultimately claimed the lives of 16 people that day.

Second to preventing injuries and saving lives this research tied severe weather patterns in Arkansas to topography in a regional way that answered questions proposed by previous researchers. Patterns were observed in the weather data that appeared influenced by topography related to the Ouachita Mountains. Regression analysis confirmed these hypotheses and strongly indicated these pervasive patterns mean Arkansans will have to endure perpetual risk. Hence, the imperativeness for quality research as a foundation for state level hazard mitigation.

CHAPTER 2

Nat Hazards <https://doi.org/10.1007/s11069-018-3201-7>

A NOVEL TRIGGERLESS APPROACH FOR MASS WASTING SUSCEPTIBILITY MODELING APPLIED TO THE BOSTON MOUNTAINS OF ARKANSAS, USA

Kyle W. Rowden and Mohamed H. Aly

Received: 26 September 2017 / Accepted: 1 February 2018
© Springer Science+Business Media B.V., part of Springer Nature 2018

ABSTRACT

This research deploys a novel mass wasting susceptibility modeling approach for cases where temporal information is unavailable, and circumstances are prejudiced to merit applying traditional susceptibility modeling strategies. Conventional models typically employ approaches deemed problematic for this study, e.g. biased weighted input; a “more is better” approach pertaining to voluminous inputs; neglecting geologic structural influence, and establishing temporal linkages between cause (trigger) and effect (failure) with a trigger being defined as a catalyst for failure, such as timed events like earthquakes or precipitation as well as physical changes like vegetation removal or slope disturbance. Road bias may also influence modeling dramatically when event data are derived from observations of road related failures, which become unreliable at predicting susceptibility in regions with no roads. However, a triggerless approach can extrapolate naturally occurring susceptibility via priori knowledge of local topography and structural geology factors. Two models are then created for comparison: one model has integrated Empirical Bayesian Kriging and fuzzy logic considering basically local topography and structural geology, while the second model has employed a standard implementation of a weighted overlay using all available (8) input data layers. Statistical comparisons show that the first model has

identified ~83%, compared to only ~28% for the latter model, of the 47 documented mass wasting events in the selected study site. These results demonstrate that the introduced triggerless approach is efficiently capable of modeling mass wasting susceptibility in areas lacking temporal datasets, which in turn can help in mitigating future geohazards.

Keywords Geohazard • Mass Wasting • Susceptibility Modeling • Analytical Hierarchy Process • Fuzzy Logic • Arkansas

INTRODUCTION

It is common for susceptibility models (SM) to make use of as many inputs as available, operating on the underlying assumption that the more inputs, the better the results (e.g. Carrara 1983; Carrara et al 1999; Daneshevar 2014; Burns and Mickelson 2016; Kirschbaum et al. 2016). Traditional approaches for modeling mass wasting hazards may still achieve viable results even though they might ignore geologic discontinuities; however, a simple approach that considers local structural geology may achieve better results. Geologic discontinuities are structural vulnerabilities in the integrity of a planar rock surface and may include: faulting, foliations, jointing, and bedding plane orientation (Singhal and Gupta 2010). In fact, neglecting the influence of bedding dip amount (DA) and dip direction (DD) may suppress the overall success of any type of mass wasting susceptibility model (MWSM), as demonstrated in figure 1. Therefore, bedding plane attitude is being considered in this research as a significant factor influencing mass wasting events (MWE).

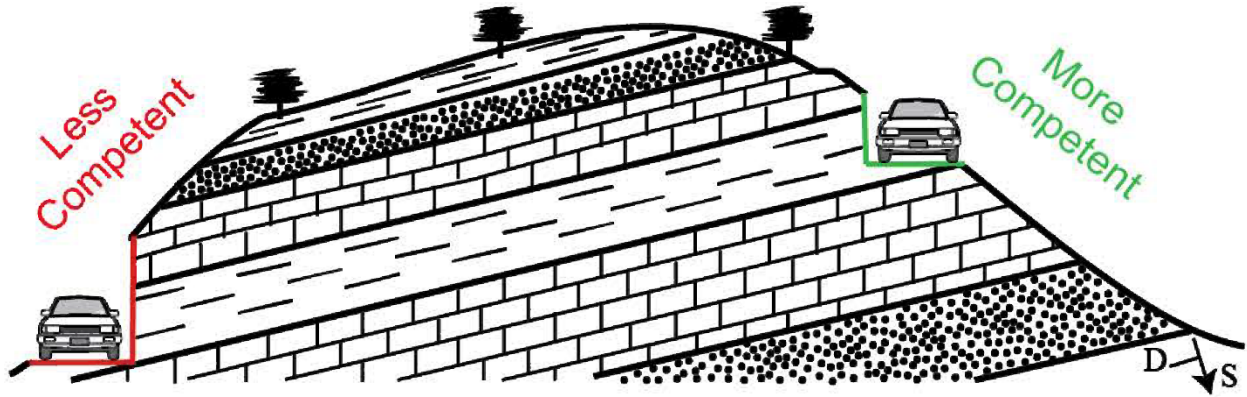


Fig. 1 Orientation of dipping strata can make a slope either more competent or less competent. Roads excavated at the down-dipping end are inherently more prone to rotational falls, block slides, and inevitable creep ultimately compromising the strength and integrity of the roadway with strike (S) and dip direction (D).

The Boston Mountain Region (BMR) is an ideal study site for testing the introduced triggerless approach for mass wasting susceptibility modeling because the local geology and structure are relatively simple. During the Ouachita Orogeny (~270 mya) Paleozoic strata of the BMR was uplifted by the north-northwestern vergence of the South American Plate in relation to the North American Plate known as Laurentia (Kluth and Coney 1981; Arbenz 2008; Keller 2012). Although heavy folding occurred in the Ouachita Mountains, about 50 km to the south - the BMR had already been uplifted into a plateau and although the southern flank was modified along the MFZ, the interior geologic setting was left relatively undisturbed. Structural characteristics in the BMR can be summarized as a region of relatively flat lying, gently deformed, detrital Pennsylvanian strata, underlain by unconformable dominantly non-detrital Mississippian formations (Zachry 1979; Zachry and Sutherland 1984). Regional dip to the south ranges from 3° to 19° with an average of about 5° (Chinn and Konig 1973; Braden and Smith 2004; Cohoon 2013). Gentle deformation in strata stair-step away from the Pre-Cambrian basement core of the Ozark Dome (Arbenz 2008) occasionally produced dip inclinations >15° to the south. A laterally extensive fault system, known as the Mulberry Fault Zone (MFZ), delineates much of the southern

boundary for BMR (e.g. Zachary and Sutherland 1984; Link and Roberts 1986; Pontiff 2007) but faulting within the interior highlands of the BMR in proximity of the study area is sparse. It is worth noting that evaluation of MWE locations to proximity of faults found no direct correlation; therefore, local faults were not considered as an influencing factor in developing our modeling procedure.

An approximately 1,200 km² study area in BMR, with a relatively consistent geology avoiding complex structures on the peripheries and providing modes of anisotropic discontinuity such as changes in geologic formation, DD, and/or DA, has been selected for this research. This is crucial for our developed triggerless approach as DA and DD can be modeled through existing data with relative ease and structural characteristics present in the subsurface that might be inherently affecting regional susceptibility can be analyzed. DD intrinsically may lead to a more competent slope (up-dip) or a less competent slope (down-dip) when considering building a road on or excavating in inclined strata, as shown in figure 1.

The aim of this paper is to develop a MWSM approach that can be applied not only to the specifics of Boston Mountains in Arkansas, but also to other regions, with similar geologic setting, experiencing mass wasting and lacking temporal datasets. Simplistic minimalist inputs applied in this research can definitely provide an efficient and effective solution. Research objectives are accomplished through a multi-faceted process involving interpolation and fuzzy modeling and the workflow (Fig. 2) can be broken into: (1) preparing necessary inputs including detailed MWEs, (2) reclassifying and converting geologic attitudes into a pseudo-structural layer (PSL), (3) interpolating and triggerless modeling, and (4) highlighting zones of potential failure for hazard mitigation. Ultimately, a statistical comparison is conducted between our new approach (model α) and a conventional weighted overlay (WO) (model β) to validate the efficiency of our triggerless

approach. Both models have particular strengths and weaknesses as explained, but results indicate that model α is superior to model β with regards to prediction accuracy.

MASS WASTING INVENTORY FOR NW ARKANSAS

All types of MWEs are considered in this research. These include, but are not limited, to rockfalls, rock topples, slumps, block slides, varying degrees of flows, and creep. Sporadic and localized case studies dealing with landslides have been conducted by the Arkansas Geologic Survey (AGS) (e.g. McElwaine 1966; McFarland and Stone 1981,1995; Bush and McFarland 1984, 1992; McFarland and Hanson 2005; Howard 2008, 2009). Extensive research by Baker (2013) used a modified version of the Selby Numerical Model (1980) and cataloged 2,000+ outcrops in central Arkansas. Man-made features accounted for 77 failures as well and are compiled into the current MWE database.

Perpetual road failures along numerous transportation corridors bisecting the BMR have resulted in restricted flow of commerce. Following Baker's (2013) study, Arkansas Department of Transportation (ArDOT) maintenance crews conducted a statewide audit of failures along Arkansas roadways and added 321 MWEs to the database. Events recorded by ArDOT span 2013-2016, but for unknown reasons MWEs related failure recorded around the beginning of the audit lack definitive dates defining the impetus for working around trigger correlated causality. An additional 14 MWEs, consisting of landslides or rock falls, were found from photogrammetric analysis and field surveys as part of the field research for this study. MWEs are mainly confined to Boston Mountains/Ozark Plateau and Arkansas River Valley physiographic regions with a minimal percentage in the Ouachita Mountains. Unconsolidated and flat lying quaternary deposits

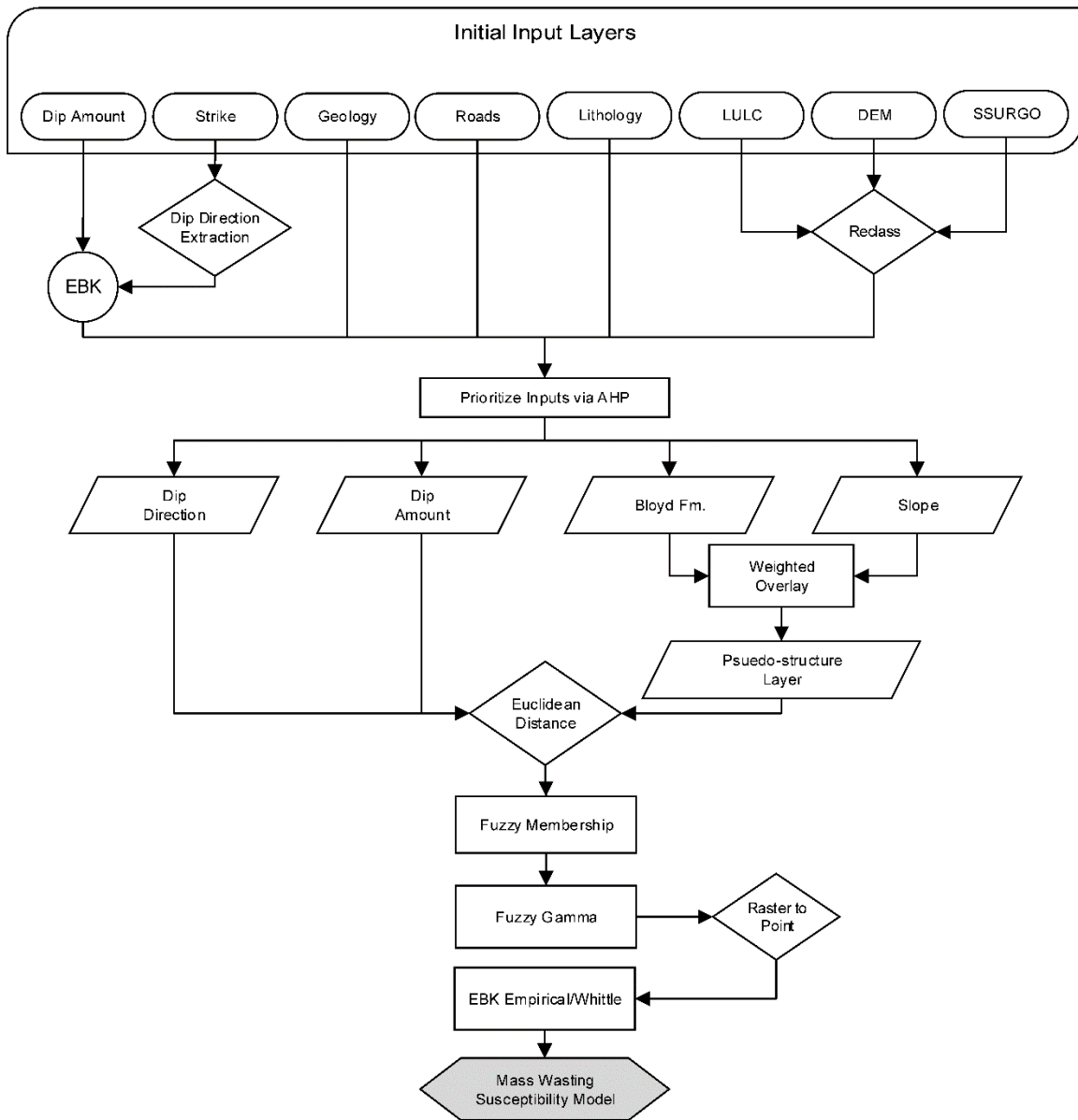


Fig. 2 Flowchart for the overall process of creating the final triggerless mass wasting susceptibility model (MWSM). Denotation for abbreviations are: Landuse/landcover (LULC), digital elevation model (DEM), soil survey geographic database (SSURGO), Empirical Bayesian Kriging (EBK), and Analytical Hierarchy Process (AHP).

in the eastern Mississippi River embayment or West-Gulf coastal plain physiographic regions pose minor stability issues relative to roadways. For this reason, all physiographic regions outside the BMR are not being considered in this research.

An unabridged mass wasting index was compiled from all available Arkansas datasets, totaling 423 locations (Fig. 3). Current density of MWEs is inconsistent with historical USGS landslide SM produced by Radbruch-Hall et al. (1982) and later digitized by Godt (1997). This model falls short in addressing inherent risk, with minimal to no recent MWE occurring in areas designated as having the highest incidences of landslides. An overview of Godt's product with the current extent of MWEs (Fig. 4)

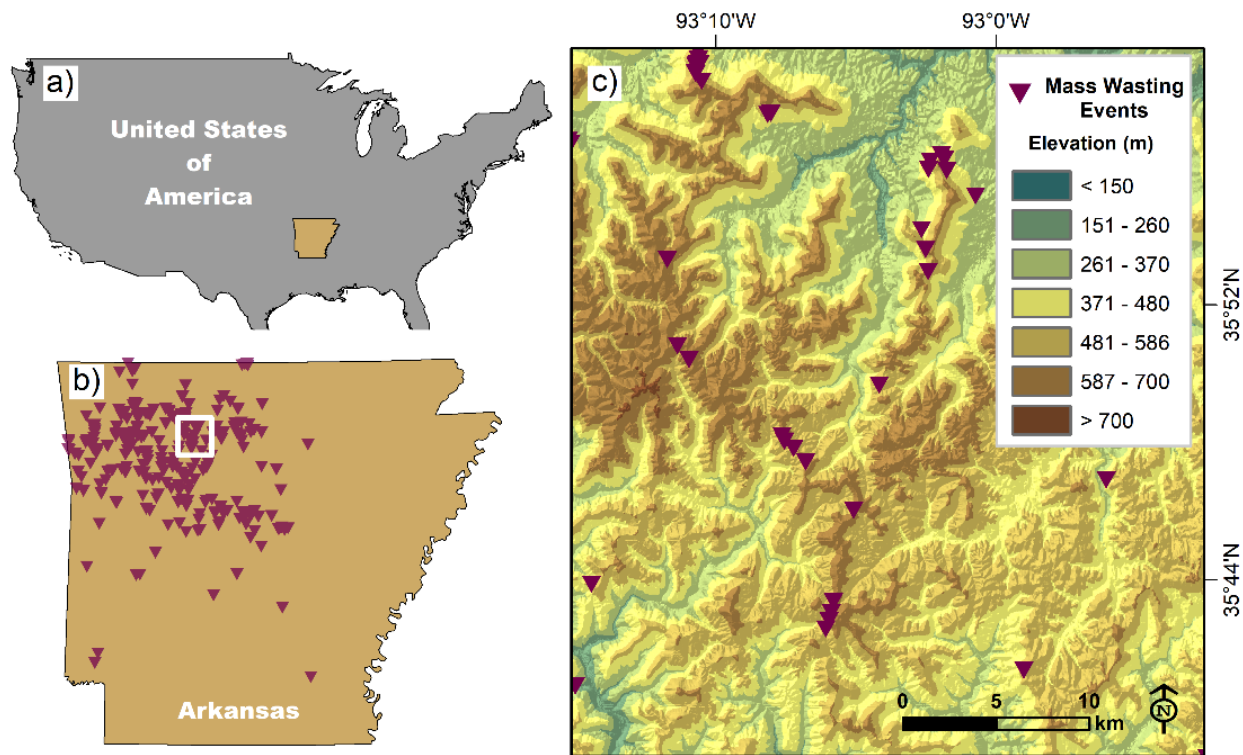


Fig. 3 Relative location of Arkansas (a) displaying distribution of mass wasting inventory (small triangles) across the state (b) and contained within the study area (c)

indicates these flagrant disparities and highlights the accuracy and unique contribution of our new model for NW Arkansas.

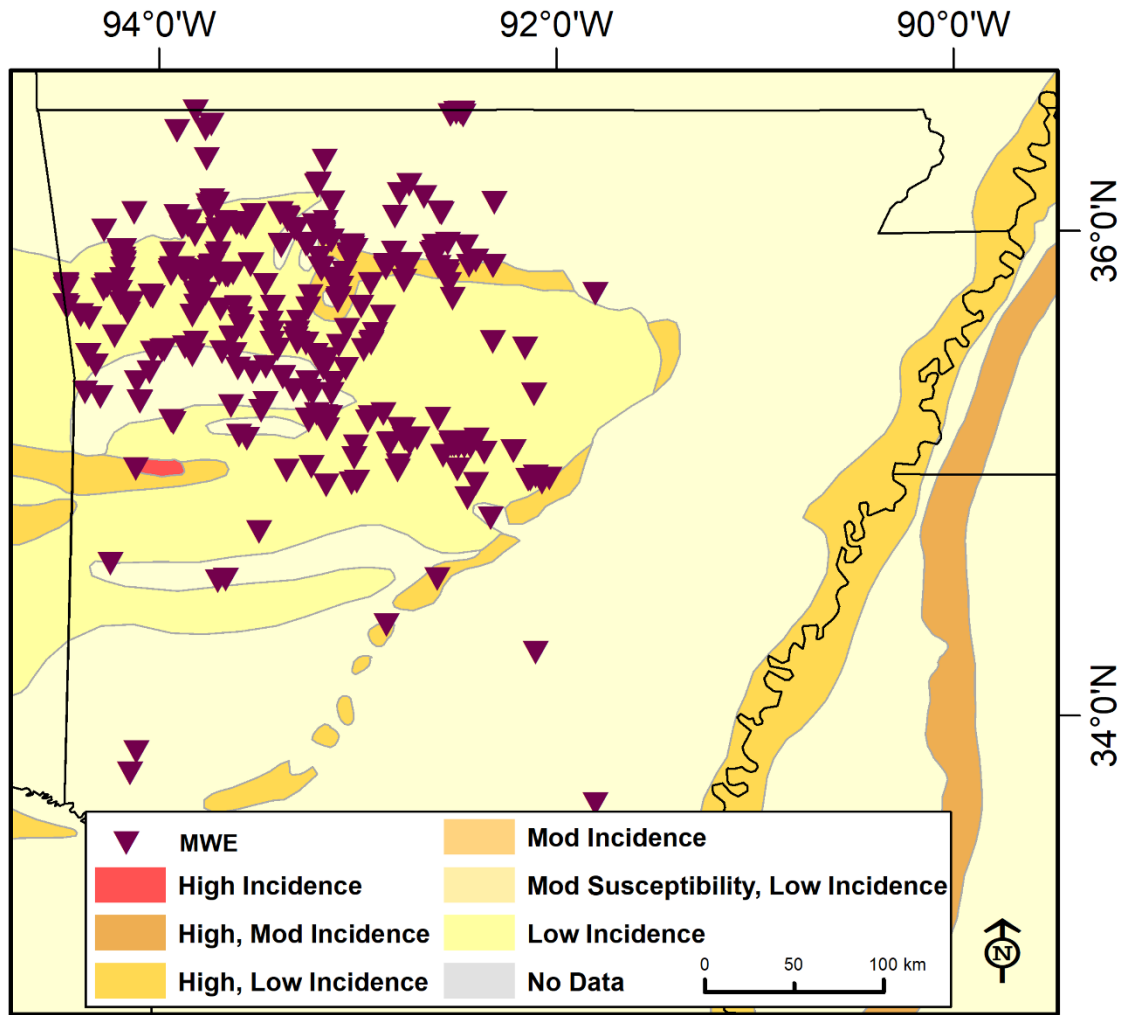


Fig. 4 Arkansas mass wasting events (pyramids) highlighting disparity of distribution and density of events with the USGS landslide susceptibility map adapted from Godt (1997).

DATASETS

The backbone of this geospatial analysis relies on developing a PSL from field surveyed geologic attitudes of strike and dip measurements. GIS layers of Arkansas geologic attitudes and their attributes are presently unavailable to the public, but thankfully provisional GIS data were supplied by AGS to facilitate this research. These provisional GIS layers contain geologic

formations as digitized polygons and extensive field measurements in the attribute tables. An assortment of detailed (15-minute) geologic maps being bisected by Arkansas Scenic Highway 7 are mosaicked together to cover the entire study site. Road failures related to MWEs over the past decade are locally well-known within the extent of the selected study area. Figure 5 shows an example of perpetual mass wasting problems along Arkansas Highway 7 adjacent to Round Mountain and immediately south of Jasper, Arkansas.

Numerous datasets are retrieved from the Arkansas Spatial Data Infrastructure (ASDI) – formally GeoStor – and are listed in Table 1. Main vector data includes: (1) SSURGO soil data defining 1500+ variances in soil types developed by the United States Department of Agriculture (USDA) and the Arkansas Natural Resources Conservation Service (ANRCS). For ease in processing and manageability, the soil data are clipped to the study area and re-classified as either ‘mountain’ soil types or the reciprocal ‘valley’ soil types. (2) Roads layer created by ArDOT and buffered into four classes of <100, 100-200, 200-300, and >300 m. (3) Geologic layers provided by AGS. (4) Geologic attitudes provided by AGS as vector points with associated attribute tables. (5) Lithology layer obtained from the United States Geological Survey (USGS). In addition, raster data include: (1) 1-arc second digital elevation model (DEM) developed by USGS, which is used to generate the slope model. (2) Landuse/landcover (LULC) created by the University of Arkansas’



Fig. 5 Riprap with steep angle of repose, part of the most recent mitigation effort to a historically problematic failure zone along Arkansas Highway 7, looking north toward Jasper (a) and looking south uphill (b) with the summit of Round Mountain immediately west

Center for Advanced Spatial Technologies (CAST), which is classified into seven classes: barren, buildings, forest, grass, roads, shrub, and water.

Table 1 Datasets used in the preliminary assessment of input variables, with abbreviations denoting Arkansas Geological Survey (AGS), landuse/landcover (LULC), Center for Advanced Spatial Technologies (CAST), Arkansas Spatial Data Infrastructure (ASDI), Arkansas Department of Transportation (ArDOT), soil survey geographic database (SSURGO), United States Department of Agriculture (USDA), Natural Resources Conservation Service (NRCS), and digital elevation model (DEM)

Layer	Dataset	Resolution/Type	Extent	Source
Geologic Formations	15-Minute Quadrangle	Polygons	Central Arkansas	AGS
LULC	Created by CAST	1-arc second (~30x30 m)	Statewide	ASDI (2006)
Lithology	Derived from USGS sources	Digitized field maps in polygons	USA	USGS (2000)
Roads	Extracted from ArDOT shapefiles	Functional Class Inventory	Statewide	ArDOT
Strike/Dip	1;52,000 Geologic survey, 1729 points	Vector layer	39°15'W – 92°45'W	AGS
Soil	SSURGO	Vector	Statewide	USDA/NRCS
Slope	Generated from DEM	1 Arc Second (~30x30 m)	Statewide	USGS
Inventory of Mass wasting events (MWE)	(322) ArDOT inventory (8) case studies (77) case study (14) surveyed	Points Points Points	Statewide Statewide Central Arkansas Boston Mountains	ArDOT AGS Baker (2013) In Situ

METHODS

DEFINING DIPS

Constructing PSL begins with geologic attribute tables containing strike and DA measurements. Attitudes have been converted into two separate layers: (1) DD and (2) DA. Standard convention in the United States defines strike with adherence to the “right hand rule”

where strike is the azimuthal direction 90° counter-clockwise to the direction of dip, with a stratum's dip being the direction in which water will flow unencumbered across a planar rock surface (Compton 1985). The geodatabase provided by AGS contains 783 attitudes within our study area.

Through simple arithmetic, a strike azimuth can be converted to DD as follows:

$$D = S + [90], \quad (1)$$

where D is the direction of dip, and S is the azimuthal direction of strike.

Initial strike azimuthal directions $>270^\circ$ produce DD values beyond 360° , which are reclassified to respective values ranging from 1° to 89° . DD reclassified values that are represented as vector point data are interpolated using EBK, and then the interpolated DD are re-classified into 16 categories combining complimentary pairs of 22.5° division. Values are grouped as $(337.5^\circ-360^\circ)$ and $(0^\circ-22.5^\circ)$ to characterize dips to the north. This process allows cardinal directions for north, northeast, east, southeast, south, southwest, west, and northwest to bisect the reclassified DD.

Similarly, DA values are processed with EBK. DA values are categorized similar to dip angles corresponding to intensity and are defined with AGS field surveyed thresholds using intensity values as the following: gentle = $3.6^\circ-7.5^\circ$, moderate = $7.6^\circ-9.2^\circ$, intermediate = $9.3^\circ-13.1^\circ$, and steep $>13.1^\circ$. Later, both DD and DA layers are joined together with WO to create our PSL that is displayed in figure 6. Dips in the immediate vicinity of faults tend to be the steepest with 19:783 attitudes exhibiting vertical orientation. Vertically oriented dips strongly influence nugget effects in kriging, a phenomenon often generated by outliers in the dataset. Kriging nugget effects are explained in great detail by Krivoruchko et al. (2006).

EMPIRICAL BAYESIAN KRIGING

Kriging is a common interpolation method developed by Levy Gandin (1959) that statistically interpolates optimal predictions filling in the gaps in spatial data. Kriging interpolates counterfeit values with varying precision based on observation inputs (e.g. Journel 1983; Kulkarni 1984; Omre 1987). Following Omre (1987), Bayesian kriging can be created by taking the kriging method and implementing a Lagrange minimization procedure. Empirical Bayesian Kriging (EBK) relies on exact interpolations derived from inputs based on empirical observations (Krivoruchko 2012), and outputs are predicted surface models where decision points run through empirical observation inputs that are unencumbered by the interpolated postulate. Consistency is guided by estimations from variogram functions, which makes the EBK method ideal for modeling areas containing dense data points (Omre 1987). These strengths make EBK a choice method for geologic interpolation. Omre (1987) expresses EBK as:

$$\sum_i \alpha_i [\gamma_{z|M}(X_i - X_j) + \gamma_M(X_i, X_j)] + \beta_1 = \gamma_{z|M}(X_0 - X_j) + \gamma_M(X_0, X_j), \quad (2)$$

where $j = 1, \dots, N$, $\sum_i \alpha_i = 1$, and $\gamma_{z|M}(X_i - X_j)$ are the variance in estimations for unknowns across the difference between field values X_i and X_j , $\gamma_M(X_i, X_j)$ is the variogram for a known

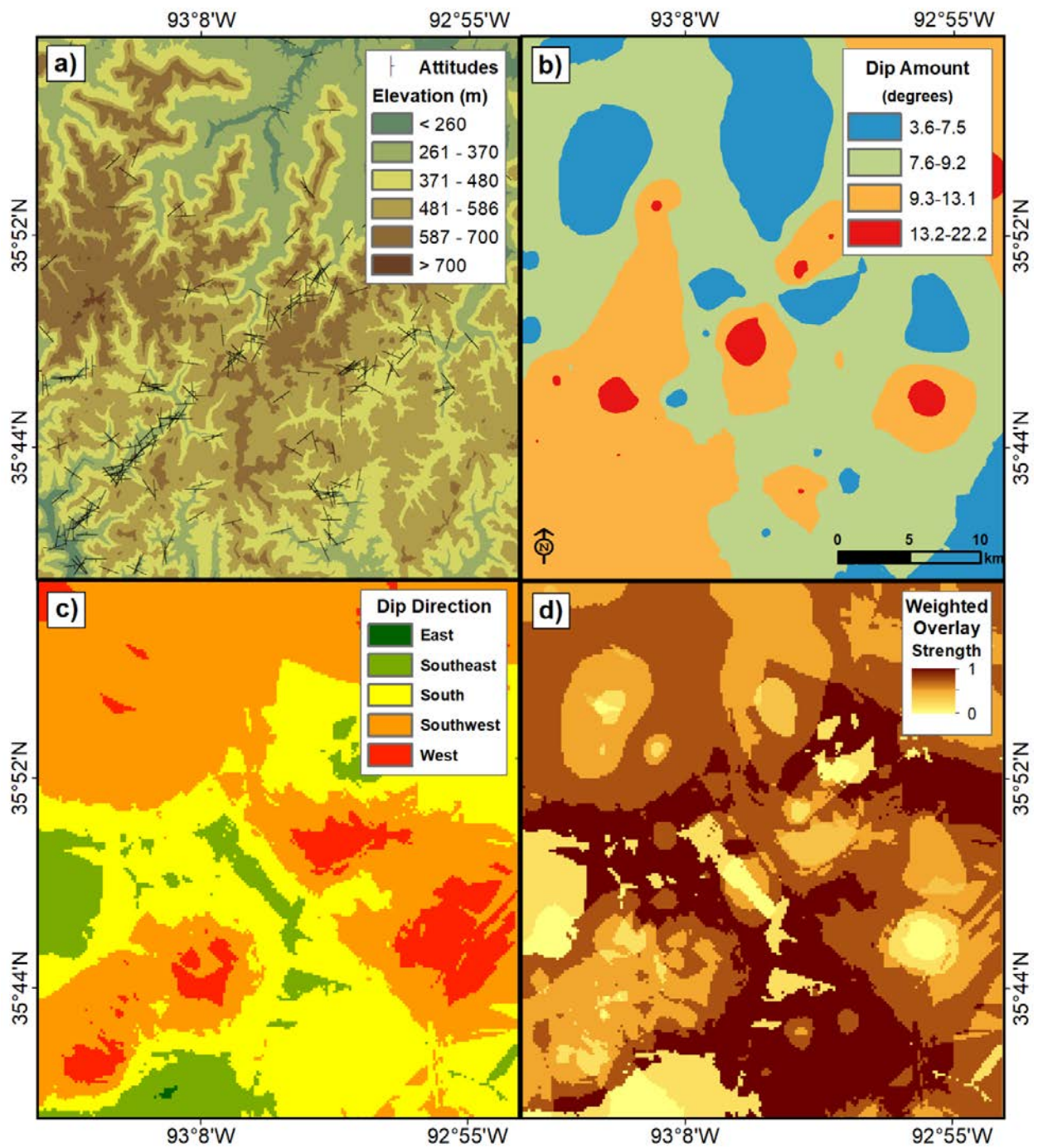


Fig. 6 (a) Geologic attitudes, (b) Empirical Bayesian Kriging (EBK) modeled dip amounts, (c) EBK modeled dip directions, and (d) Weighted overlay pseudo-structural layer created for triggerless modeling

priori evaluated across field values of X_i and X_j , β_1 is a Lagrange multiplier, and X_0 is an independent third location.

A lemma for when location of independent weights becomes unconstrained from X_0 locations is defined by Omre (1987) as being:

$$\beta_1 = C + \left[\frac{\sigma_M^2(X_0)}{2} \right], \quad (3)$$

where C is a constant brought into the equation, and σ_M^2 is the variance in the interpolation evaluated from the third location.

CONDUCTING ANALYTICAL HIERARCHY PROCESS

Quantitative evaluation of qualitative observations often times becomes the crux when working with subjectively perceived hazard scenarios (Kirschbaum et al. 2016). One common solution for priori observations is to implement a pairwise comparison using the analytical hierarchy process (AHP) matrix. A pairwise comparison matrix based on the scale shown in Table 2 enables weighting variables, and comparisons can be assessed to a level of consistency (e.g. Aly et al. 2005). AHP, developed by Saaty (1977), computes the consistency ratio (C_R) and use it as a consistency index (C_I). C_R serves as a critical statistical check to verify whether the pairwise comparisons are generated through random assignments of weights (Saaty 1977) and can be established as follows (e.g. Saaty and Vargas 1991):

$$C_R = C_I/R_I, \quad (4)$$

where R_I is the resulting (consistency) index, dependent on Saaty's (1977) matrix order. C_I is the consistency index that is commonly expressed as:

$$C_I = (\lambda_{max} - n) / (n - 1), \quad (5)$$

where the principle or largest eigenvalue calculated from the matrix is represented by λ_{\max} and n denotes the order of the matrix.

Table 2. Pair-wise comparison scale

Ranking Hierarchy	Importance	Definition
1	Equal	Comparisons between objectives are essentially equal
3	Moderate	Slight favoritism between compared objectives
5	Strong	Strong favoritism between compared objectives
7	Very strong	Favoritism between compared objectives
9	Extreme	Most confident assertion of highest order value
2,4,6,8	Intermediate weight	Middle point compromise between ranking integers
1/9,1/7,1/5,1/3	Reciprocal values	Serve as the inverse comparison juxtaposed to integers

Typically, any $C_I \leq 0.10$ will suffice as a reasonably acceptable consistency level. Pairwise matrices generating C_I 's > 0.10 exhibit too much random inconsistency and require re-evaluation (Saaty 1977). For the initial AHP pairwise matrices determining which variables might be considered for the final model, all C_I 's have values < 0.08 . Comparisons using AHP are conducted on the eight inputs and weights are assigned accordingly. Preliminary modeling results have indicated that the eight influencing factors have watered down the severity of the region, thus a conclusive decision has been made to discard all triggers, and hence the precipitation variables are not considered for further processing. Major contributing non-trigger factors have become the

focus of the modeling and three inputs, including the Bloyd geologic formation, slopes greater than gentle, and the geologic PSL, are considered for the remaining analyses.

WEIGHTED OVERLAY ANALYSIS

Integration of multi-criteria evaluation into GIS has been a time proven strategy for complicated spatial problem solving since the near inception of GIS (e.g. Keeney and Raiffa 1976; Nijkamp 1980; Voogd 1983; Carver 1991; Shahabi and Hashim 2015). ESRI, the creator of ArcGIS software used in this research, refers to weighted linear combination for multi-criteria modeling as a Weighted Overlay (WO) process that works on theorems developed by Voogd (1983) for weighting linear combinations. Superficially, WO is analogous to AHP weighting, but WO in ArcGIS cannot account for non-statistically viable bias that ultimately ends up influencing the outputs. In this research, all weights applied in any WO process are cross-checked via an AHP matrix to ensure acceptable C_I values are present and to justify any priori weighting applied to a WO process. Weight applied to each factor results in the summation of a suitability or susceptibility output. WO is actually an easy means to facilitate AHP weighting in GIS, and therefore both techniques are used in concert. Eastman et al (1995) are credited with the summation defined as:

$$S = \sum_{i=1}^n (W_i * X_i), \quad (6)$$

where S represents the suitability (susceptibility), W_i stands for factor I 's weight, and X_i denotes factor i potential rating.

Slope and Bloyd formation inputs are reclassified with Boolean assignment into two categories. Slopes: > gentle slopes = 1 and gentle slopes = 0. Bloyd formation: Bloyd Fm. = 1 and Non-Bloyd = 0. Coding pixel values as 1's and 0's denotes whether an input has any importance

at all (1) or no importance (0). A modified version of Eastman et al. (1995) suitability equation has been applied to these Boolean constraints layers:

$$S = \sum_{i=1}^n (W_i * X_i) * \prod C_j, \quad (7)$$

where \prod denotes the major product operator, and C_j represents the potential score constrained by j . Cartographic outputs for permutations involved in the PSL process are shown in Figure 6.

FUZZY LOGIC AND MEMBERSHIP TRANSFORMATIONS

Calculating Euclidean distance is a critical initial step for fuzzy modeling. The Euclidean distance, which is the shortest distance between two points, is computed for all six chosen variables. All roads and mass wasting locations within the study area are selected and Euclidean distances are calculated. Slopes are categorized into four groups corresponding to the angle of slope: gentle slope ($<7^\circ$), moderate slope (7.1° - 15°), intermediate slope (15° - 30°), and steep slope ($>30^\circ$). Slopes greater than 7° have increased potential for failure, therefore Euclidean distance is calculated based on Gentle Slope ($<7^\circ$), where reciprocal value represent all slopes with risk. The final two Euclidean distance layers were created for the Bloyd Formation and the Atoka Formation. These two Pennsylvanian formations are shale dominated with massive sandstone members and together account for a significant percentage of MWEs (Cohon 2015).

Discrepancies, inconsistencies, and biases are expected hindrances with SM, and thus great care must be taken by the analyst to mitigate output degradation (Kirschbaum et al. 2016). Fuzzy logic is a method for assigning a continuum of values ranging from 0 to 1, developing a membership where each member can be related by complement, convexity, inclusion, intersection, relation, union, or a plethora of other relations (Zadeh 1965). A conversion process takes place, often algebraically in the form of a “fuzzy membership function” (Bonham-Carter 1995). These

new input layers, representing possibility, can be created using either numerical data or statistical methods (Kirschbaum et al. 2016). In this study, AHP has been used to rank the multi-criteria factors and then the significant contributing non-trigger variables are fuzzy modeled.

Previously calculated Euclidean distances are the main inputs for the fuzzy memberships. Fuzzy membership transforms input data to fit within a range from 0 to 1 based on probability that any member might be found within a specific set. Fuzzy members not found within a specific set are given a value of 0. Conversely, fuzzy members falling within a specific set are assigned a range >0 and ≤ 1 , where absolute certainty is defined as 1.

Analogous to Zadeh's (1965 and 1968), fuzzy algorithms have been applied to this study through ESRI's fuzzy large and fuzzy near transformations. Fuzzy large is the optimal choice when the memberships approach 1, and thus it is applied to slopes $>$ gentle. Fuzzy large is defined by ESRI (2016) as:

$$\mu(x) = \frac{1}{1 + \left(\frac{x}{f_2}\right)^{-f_1}}, \quad (8)$$

where f_1 represents member spread typically ranging between 1 and 10, f_2 is a user-defined midpoint value, with ESRI's being 0.5.

Fuzzy near transformation is a function where the membership ends up falling near a particular value where the midpoint is user-defined with a membership of 1 and the spread ends up decreasing to 0. Therefore, fuzzy near is the optimal function to use with our PSL and Bloyd formation inputs. Fuzzy near is expressed by ESRI (2016) as:

$$\mu(x) = \frac{1}{1 + f_1 * (x - f_2)^2}, \quad (9)$$

where f_1 represents the spread of members that typically ranging between 0.001 and 1. Like fuzzy large, f_2 is a user-defined midpoint value for a fuzzy membership of 1.

Fuzzy overlay is the last step in the fuzzy logic process, where all fuzzy membership possibility layers are combined together into one final output. Fuzzy locations with possibly values ≥ 0.5 are considered susceptible to a MWE, thus fuzzy gamma overlay is applied in this case. Fuzzy gamma is defined by ESRI (2016) as:

$$\mu = (1 - \prod_{i=1}^n (1 - \mu_i)^\gamma) \times (\prod_{i=1}^n \mu_i)^{1-\gamma}, \quad (10)$$

where μ represents pixels with high susceptibility for mass wasting, μ_i is any likelihood a MWE might occur relative to variable i , n represents the number of variables being combined, and γ defines a parameter describing the highest or the lowest degree any input might be manifested into the fuzzy overlay output.

Fuzzy gamma overlay establishes a multicriteria input relationship between possibility and examination of relationships without reliance on a single membership (ESRI 2016). Fuzzy gamma overlay is applied to the three fuzzy memberships to create the first part of the SM, and ultimately raster values are converted to points suitable for EBK interpolation. Raster attribute tables are built for models α and model β , enabling geometric interval classification of susceptibility risk into six risk classes. Figure 7 displays a diagrammatic workflow for all the processes and transformations that have been automated using ESRI's model builder for expedience and replicability aiding heuristic exploration and analysis.

NORMALIZATION

Pixel values for each respective output are normalized providing a base for later quantitative comparison between our triggerless model and a conventional model. The final output

of each model is classified into six respective categories using geometric classification for distinguishing susceptibility risks as: low, low-moderate, moderate, moderate-high, high, and very high. Geometric interval classification serves as a compromise between quantile separation and natural breaks (ESRI 2016). Each class is evaluated using an adaptation of the Salciarini et.al (2017) approach to determine pixel value performance:

$$\rho, \alpha = \frac{(T_c)(A_c)}{R_a}, \quad (11)$$

where T_c delineates the total numbers of cells, A_c is the relative pixel area, and R_a is the grid area for the extent of the model and ρ is the efficacy evaluation metric for each relative risk class pixel count.

Next, an average of MWE's per class is found where ρ_a represented each class average:

$$\rho_a, \alpha = \frac{N_{mwe}}{N_{tot}}, \quad (12)$$

where N_{mwe} stands for the number of MWEs occurring within each class, over the total 47 MWEs for the entire study area, N_{tot} .

Final normalization is computed through the difference of equations (12) over (11) as a measure of specific MWE densities per class defined by

$$\psi, \alpha = \frac{\rho_a, \alpha}{\rho, \alpha}, \quad (13)$$

Each quantity for da, α , ρ_a , and ρ, α represents the spatial distribution apparent for each class. The same process is used for normalization of model β . Both methods represent all MWE within models because all blank values in the WO method are reclassified to correspond with the low risk class.

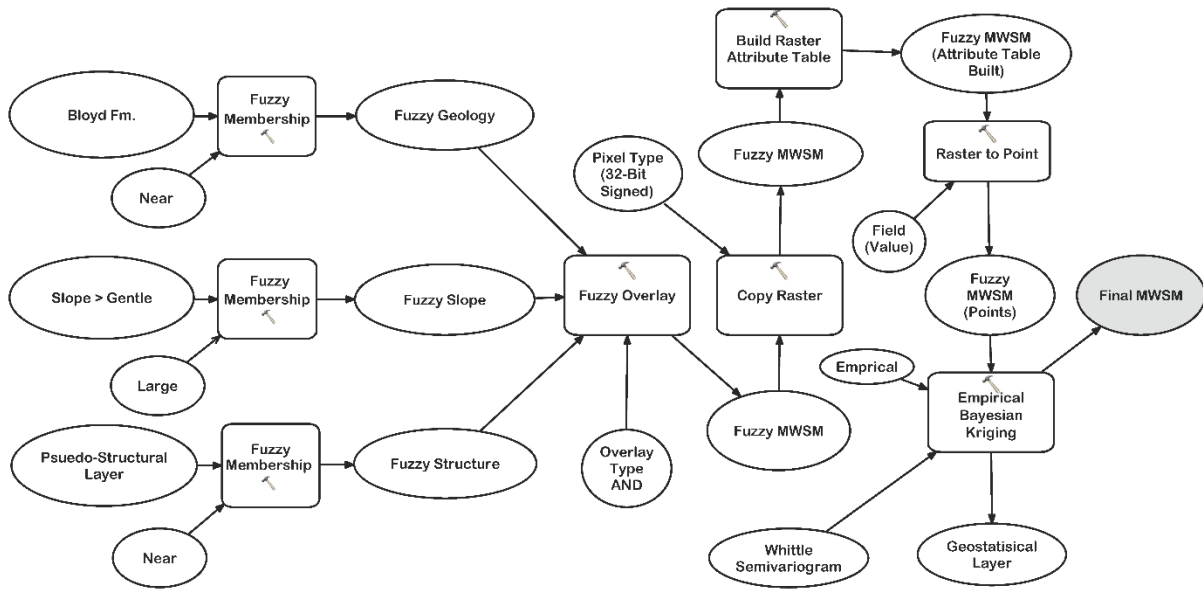


Fig. 7 ArcGIS model builder diagram for the mass wasting susceptibility modeling, beginning with critical inputs previously determined through the Analytical Hierarchy Process of priori knowledge where the Bloyd Fm. is geologic formation with most influence, all slopes > gentle (gentle being $<7.5^\circ$), and the pseudo-structural layer (referred to as PSL in text).

SPATIAL AUTOCORRELATION

Statistical comparisons between attribute values and feature locations are obtained by means of spatial autocorrelation (SA), utilizing Global Moran's I . SA works on the premise of Tobler's Law (1970) which states that near features are more closely related than features further away. Along with Moran's I , both a p-score and a z-score are calculated as means of determining whether the complete spatial randomness null hypothesis can be rejected or not. Significance level (p-score) is a percentage of probability that clustering is related to an underlying spatial influence. P-score values range from 0.01 to 0.10 on the weak probability end and 0.01 to 0.01 on the strong confidence end. Small p-scores imply spatial patterns being observed are not from random processes. Z-scores are critical scores representing standard deviations and combined with corresponding p-scores constitute confidence. Z-scores range from <-2.58 with weak confidence

up to >2.58 for strong confidence. Z-scores ranging from -1.65 to 1.65 constitute represent the *null* hypothesis (Table 3). Moran's I is computed as (ESRI 2016):

$$I = \frac{n \sum_{i=1}^n \sum_{j=1}^n W_{i,j} z_i z_j}{S_0 \sum_{i=1}^n z_i^2}, \quad (14)$$

where the attributes deviation of any feature i from mean ($x_i - X$) is z_i , total count of features is n , spatial weight between (i, j) is $W_{i,j}$, and S_0 is the assemblage of all spatial weights:

$$S_0 = \sum_{i=1}^n \sum_{j=1}^n W_{i,j}, \quad (15)$$

Z_I-score is calculated through:

$$z_I = \frac{I - E[I]}{\sqrt{V[I]}}, \quad (16)$$

where:

$$E[I] = -\frac{1}{n-1}, \quad (17)$$

$$V[I] = E[I^2] - E[I]^2, \quad (18)$$

Attribute tables for MWE and model α now can be joined by a spatial relationship for each respective risk class based on distance in meters from each MWE. SA is then applied to the newly joined table based on 'distance' field permitting a determination that overall confidence between the relationships are not random. Autocorrelation is performed six times for the six classes at distances of: 1, 50, 100, 150, 200, and 250 m. As anticipated, a direct correlation between increased distance and increased confidence is observed.

Table 3 Associated confidence intervals relative to Moran's I for spatial autocorrelation.

Significance (p-values)	Confidence	Critical Value (z-score)
0.01	99%	<-2.58
0.05	95%	-2.88 – -1.96
0.10	90%	-1.96 – -1.65
-----	Null	-1.65 – 1.65
0.10	90%	1.65 – 1.96

RESULTS AND DISCUSSIONS

Primary inspection of model α finds distribution of risk ratings across the study area to be consistent with field observations, where the model’s moderate-very high risk classes match with in situ remarks. The opposite is true for model β because of the heavy influence of road related input bias. Steep valley walls and remote locations from roads that are expected to have considerable risk ratings are not reliably represented in model β . This is anticipated when modeling susceptibility using triggers like roads because they are narrow features and even buffering them by several hundred meters fails to enhance modeling accuracy in areas outside of the buffer zones. A substantial number of MWEs is identified in the lowest risk class of Model β , while MWEs appear well represented in the higher risk class of model α .

Additional metrics for comparison are found by applying several distinctive quantitative techniques for further analysis, and the results are consolidated in Table 4. Averages of normalized pixel count success rates show both models are near equivalent at predicting very high risk: 4.16% and 6.91% for models α and β , respectively. This is unexpected considering the heavy influence of road bias into model β and success is hypothesized to be much higher with that model per average pixel count success. When risk classes moderate through very high are considered, both

models are comparable with average pixel success being 67.84% and 68.72% for models α and β , respectively. Tertiary comparison of risk classes of low and low-moderate show a likeness at 32.16% (models α) and 31.28% (models β) normalized pixel success (Table 4).

Table 4 Normalized pixel count comparison of model success relative to geometrically classified risk categories.

Model		Low	Low-Mod	Moderate	Mod-High	High	Very High	Total
α	Tc	6182	15974	21210	9432	13226	2866	68890
	Ca	1.0000	1.0000	1.0000	1.0000	1.0000	1.0000	1.0000
	Ra	68890	68890	68890	68890	68890	68890	68890
	\cap	0.0897	0.2319	0.3079	0.1369	0.1920	0.0416	1.0000
β	Tc	115187	3147	29772	103132	100912	26147	378297
	Ca	1.0000	1.0000	1.0000	1.0000	1.0000	1.0000	1.0000
	Ra	378297	378297	378297	378297	37830	378297	37830
	\cap	0.3045	0.0083	0.0787	0.2726	0.2668	0.0691	1.0000

Accuracy for predicting number of MWEs within each risk class in both models is also analyzed. Model α has yielded only one MWE in the lowest risk class and has increased in accuracy in the higher risk classes. On the other hand, 34 MWEs are found in the lowest risk class of model β . Model β exhibited a bi-modal pattern where MWEs are only contained in the extreme classes and middle risk classes show no events. With consideration of the four highest risk classes, model α achieves an overall 82.97% accuracy versus a 27.66% accuracy for model β . Remaining realizations for low and low-moderate risk classes convey that only 17.02% of MWEs are found in these classes of model α , which is at drastic variance with 72.34% found in these lowest risk classifications for model β (Table 5).

Table 5 Accuracy comparison of model success in predicting a mass wasting event (MWE) per geometrically classified risk categories.

Model		Low	Low-Mod	Moderate	Mod-High	High	Very High	Sums
α	N_{mwe}	1	7	17	7	8	7	47
	N_{tot}	47	47	47	47	47	47	---
	\cap_a	2.13%	14.89%	36.17%	14.89%	17.02%	14.89%	100.00%
β	N_{mwe}	34	0	0	0	5	8	47
	N_{tot}	47	47	47	47	47	47	---
	\cap_a	72.34%	0.00%	0.00%	0.00%	10.64%	17.02%	100.00%

An average (ψ) of \cap over \cap_a quantifies a normalized effectiveness for each respective approach. Strengths equaling or surpassing 1.0 are being considered reliable. Model α delivers robustness across risk classes and summation of all ψ values is 7.6086. Model β scores 2.3758 for low risk and 2.4627 for very high risk, with a summation of ψ values being 5.2373 (Table 6). This can be thought of as relative strength comparison and the distribution strength for model α is juxtaposed to the inadequacies of model β (Fig. 8). A final strength check for model α , through SA, verifies that model α 's appointment of risk classes has a >90% confidence that random generation of risk classes is not occurring in its final output. SA is not performed for model β because this method already serves as a proxy for similarly established WO. SA determines likelihood that polygons in model α are not randomly assigned relative to known locations of MWEs. Referring to Table 3, confidence is >90% in all cases but drops to the lowest threshold for moderate and mod-high classes at 1 m distance, signifying the greatest potential weakness in the model. Table 7 arranges Moran's I , z-scores, and p-values for spatial distance SA strength check, and figure 9 displays a side-by-side comparison of model α and model β .

Table 6 Normalization chart comparing models α and β where pixel values have been normalized to reflect each model respective accuracy.

Model		Low	Low-Mod	Moderate	Mod-High	High	Very High	Sums
α	\cap	0.0897	0.2319	0.3079	0.1369	0.1920	0.0416	1.0000
	\cap_a	0.0213	0.1489	0.3617	0.1489	0.1702	0.1489	1.0000
	ψ	0.2371	0.6423	1.1748	1.0878	0.8866	3.5800	7.6086
β	\cap	0.3045	0.0083	0.0787	0.2726	0.2668	0.0691	1.0000
	\cap_a	0.7234	0.0000	0.0000	0.0000	0.1064	0.1702	1.0000
	ψ	2.3758	0.0000	0.0000	0.0000	0.3988	2.4627	5.2373

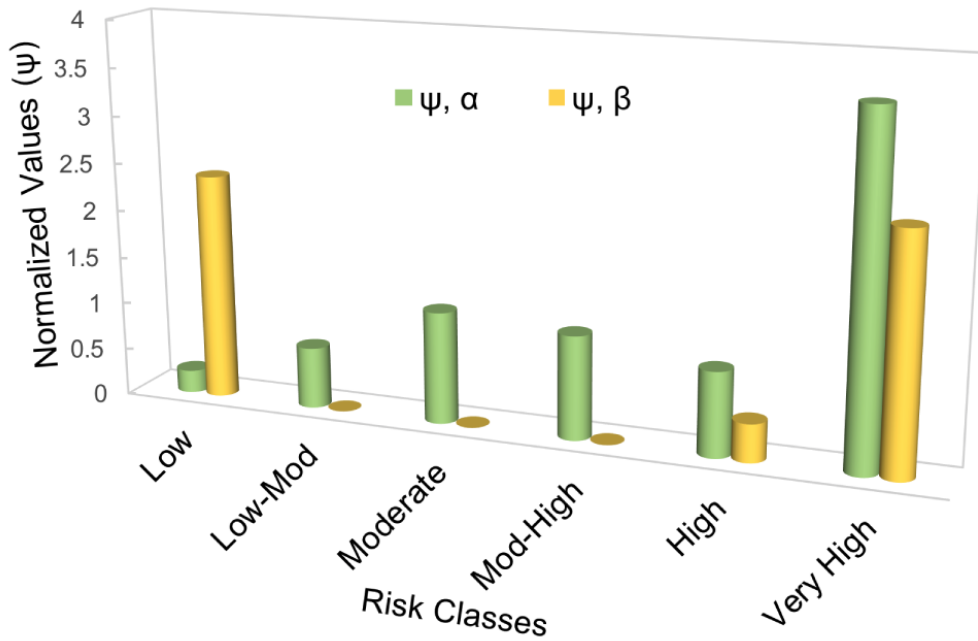


Fig. 8 Comparison of normalized (ψ) values for models α and β .

Table 7 Extracts from spatial autocorrelation conducted for model α relative to distances from mass wasting events (MWE). Model α has p-values of 0.10-0.01 and z-scores of >1.65 that indicate $>90\%$ confidence that all risk classes classified with a geometric interval classification are not by random chance, implying robustness and accuracy in applying a triggerless approach to susceptibility modeling. Model β is not considered because of inherent modeling bias in input weighting regarding roads and landuse/landcover.

	MWEs	1	7	17	7	8	7	47
Meters		Low	Low-Mod	Moderate	Mod-high	High	Very High	Averages
1	Moran's I	1.00034	0.53645	0.46944	0.46655	0.53356	0.46699	0.57889
	z-score	3.40319	1.91845	1.77420	1.74930	1.98702	1.80106	2.10554
	p-value	0.00067	0.05505	0.07603	0.08239	0.04692	0.07169	0.05546
50	Moran's I	0.98950	0.61923	0.36870	0.52896	0.62313	0.46441	0.59899
	z-score	3.38874	2.21768	1.42036	1.98868	2.32376	1.80461	2.19064
	p-value	0.00070	0.02658	0.15550	0.04695	0.02014	0.07114	0.05350
100	Moran's I	1.01763	0.66250	0.35623	0.40827	0.54820	0.42440	0.56954

In interpolation, quality is proportional to point distribution of knowns. Modeling in this research relies mainly on the 783 available geologic attitude measurements by AGS for developing a PSL. If the analyses were performed with less dense data distribution, the model's quality would most likely degrade and conversely could stand to improve in quality with greater density and distribution. The same can be said for the strategy of modeling susceptibility using fuzzy logic when converting the output into points for EBK to fill out the gaps in the study area. It is critical to have quality distribution of point density. EBK is a powerful interpolation method and it has been shown to be critical in conclusory findings of the triggerless approach.

The developed triggerless modeling approach has shown great promise in using a "less is more" technique to solve a problem with temporal limitations and the pervasive geology can be considered with an idealized scenario. However, the introduced approach may not be suitable for

applying over areas of complex geology where structural geology is heavily influenced by orogenic episodes, for instance. It has been argued (Wang and Strong 1996; Watts and Shankaranarayanan 2009; Haug et al. 2011) that limiting inputs can have negative effects on modeling, but necessary quality inputs always have priority. In this study, only the highest quality inputs with the most reliable and significant influence on causality with MWEs are used. Analysis of the triggerless model has identified numerous areas of historical events away from known roads (Fig. 9). We suggest that these areas be surveyed and monitored in the future. About 83% out of 47 MWEs fell into moderate-very high-risk classes of our triggerless model, which is far more accurate than previously published model by Radbruch-Hall et. al (1982) and Godt (1997) (Fig. 4). Certainly, the introduced triggerless approach provides good research foundation for further analysis in the future.

CONCLUSIONS

Standard practice for MWSM relies mainly on weighted trigger inputs and correlates with temporal commonality to predict failure. This approach works fine especially for timed events, but it becomes inapplicable when temporal data are unreliable or unavailable. Hurdles present in contemporary research methods regarding data limitations for modeling susceptibility are successfully overcome by creating a new PSL product of strike and dip, discarding unreliable triggers that weaken model's predictive ability with extraneous bias, and fusing fuzzy logic and EBK for triggerless modeling. Mass wasting is a prevalent geomorphic process revolving around exogenic degradation. This research argues that underlying geology accentuates mass wasting susceptibility and therefore should not be excluded as a critical input in modeling. Our new triggerless approach has successfully predicted approximately 83% of documented MWEs in moderate-very high risk classes. The developed triggerless approach has been proven to provide a

new perspective to understanding inherent risk in the BMR in northwest Arkansas and can be duplicated for modeling mass wasting susceptibility in regions with similar geologic conditions.

When a road is constructed across hilly areas, the slope is compromised and most likely becomes a catalyst for failure. The BMR is not unlike any other plateau region, where existing road infrastructure is located across and along considerable sections of various slopes. Areas which may be more inherently prone to slope failure can be identified easily across sections of roads with the highest risk classes of our model and can be targeted for further in situ analysis as well as preventative mitigation. This is crucial for the region because previous models indicate that many vulnerable areas are diluted to low risk categories, conveying a false sense of safety. Generally speaking prior to this research, a holistic catalog of MWEs in Arkansas was not existing as datasets were punctuated across various departments and institutions. Currently, our geodatabase has over 400 MWEs for future research.

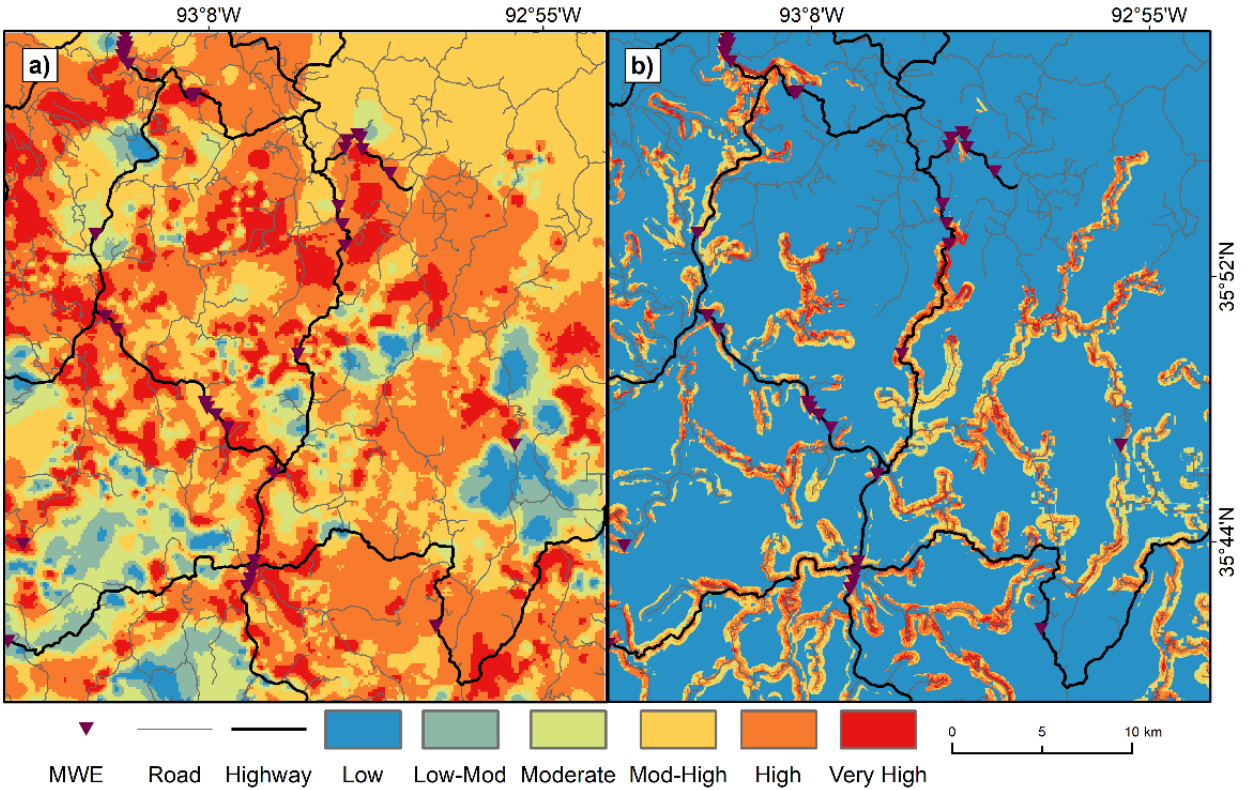


Fig. 9 (a) Triggerless model (α) employing Fuzzy logic and Empirical Bayesian Kriging (**b**) Conventional model (β) relying on weighted overlay of all available input layers where model β indicates a heavy road bias due to weighting roads as the most important factor influencing mass wasting events based on concurrent field observations

ACKNOWLEDGEMENTS

This research is funded by NASA EPSCoR RID grant #24203116UAF. Many thanks are due to Bekki White and Ty Johnson from AGS for providing access to their GIS database. The comprehensive geodatabase of this research has been established using GIS data archived at AGS, ArDOT, USGS, and ASDI. Thanks also to Martha Kopper from AGS and anonymous reviewers for their valuable comments and suggestions.

REFERENCES

- Aly MH, Giardino JR, and Klein AG (2005) Suitability assessment for New Minia City, Egypt: A GIS approach to engineering geology. *Environ & Eng Geosci* 11(3):259-269. doi: 10.2113/11.3.259
- Arbenz JK (2008) Structural framework of the Ouachita Mountains, in N.H. Suneson, (ed.), *Stratigraphy and structural evolution of the Ouachita Mountains and Arkoma Basin, southeastern Oklahoma and west-central Arkansas: Applications to petroleum exploration: 2004 field symposium*. Okla Geol Surv Circ Report 112(A):1-40
- Baker C (2013) A model for predicting bedrock failure in the Arkansas River Valley region of western Arkansas. *Ark Geol Surv MP-24*:1-28
- Braden AK, Smith JK (2004) Lurton quadrangle, Newton County, Arkansas 1/24,000. Arkansas Geological Survey. http://www.geology.ar.gov/maps_pdf/geologic/24k_maps/Lurton.pdf. Accessed 8 April 2017
- Bonham-Carter G (1994) *Geographic information systems for geoscientists*. Pergamon, New York
- Bui DT, Nguyen QP, Hoang N, Klempe H (2017) A novel fuzzy k-nearest neighbor inference model with differential evolution for spatial prediction of rainfall-induced shallow landslides in a tropical hilly area using GIS. *Landslides* 14:1-17. doi:10.1007/s10346-016-0708-4
- Burns WJ, Mickelson KA (2016) Protocol for deep landslides susceptibility mapping. *Oregon Dep Geol Miner Ind Spec P* 48:1-63
- Bush WV, McFarland JD (1984) Arlington Hotel landslide, Hot Springs, AR, prepared as a memorandum to Norman F. Williams. *Ark Geol Comm* 1
- Carrara A (1983) Multivariate models for landslide hazard evaluation. *Math Geol* 15(3):403–426. doi:10.1007/BF01031290
- Carrara A, Guzzetti F, Cardinali M, Reichenback P (1999) Use of GIS Technology in the prediction and monitoring of landslide hazard. *Nat Hazards* 20:117-135. doi:10.1023/A:1008097111310
- Carver SJ (1991) Integrating multi-criteria evaluation with geographical information systems. *Int J Geog Inf Sys* 5(3):321-339. doi:10.1080/02693799108927858
- Chin AA, Konig RH (1973) Stress inferred from calcite twin lamellae in relation to regional structure of northwest Arkansas. *GSA Bull* 84(11):3731-3736. doi:10.1130/0016-7606(1973)84<3731:SIFCTL>2.0.CO;2
- Cohon RR (2013) *Geologic Roadguide to the Scenic 7 Byway*. Little Rock, AR
- Compton RR (1985) *Geology in the field*. Wiley, New York

- Daneshvar MRM (2014) Landslide susceptibility zonation using analytical hierarchy process and GIS for the Bojnurd region, northeast of Iran. *Landslides* 11:1079-1091. doi:10.1007/s10346-013-0458-5
- Eastman JR, Jin W, Kyem PAK, Toledano J (1995) Raster procedures for multi-criteria/multi-objective decisions. *Photogramm Eng Remote Sci* 61(5):539-547. doi: 0099-1112/95/6105-539
- ESRI (2016) ArcGIS10.4.1 desktop help. <http://resources.arcgis.com/en/help/>. Accessed 15 June 2017
- Gandin LS (1959) The problem on optimal interpolation. *Trudy Glavn geofiz observatoria* 99:67 – 75
- Godt JW (1997) Digital Compilation of Landslide Overview Map of the Conterminous United States. US Geol Surv Open-File Rep 97-289
- Haug A, Zachariassen F, Van Liempd D (2011) The cost of poor data quality. *J Ind Eng and Manag* 4(2):168-193. doi:10.3926/jiem.2011.v4n2.p168-193
- Howard JM (2008) Jones landslides, Pottsville, Arkansas: 2 ½ years of monitoring. *Ark Geol Surv Spec Rep* 1-41
- Howard JM (2009) Blackjack Lane landslide on Gaither Mountain, SW of Harrison, Boone County, Arkansas. *Ark Geol Surv* 1-8
- Journel AG (1983) Fuzzy Kriging: Internal notes, Department of AES. Stanford University
- Keeney RL, Raiffa H (1976) Decision with multiple objectives: Preferences and value trade-offs. Wiley, New York
- Keller GR (2012) Overview of the Structure and Evolution of the Ouachita Orogenic Belt from Mississippi to Mexico. Presentation Tulsa Geol Soc.
- Kirschbaum DD, Stanely T, Yetheendradas S (2016) Modeling landslide susceptibility over large regions with fuzzy overlay. *Landslides* 13:485-496. doi:10.1007/s10346-015-0577-2
- Kluth CF, Coney PJ (1981) Plate tectonics of the ancestral Rocky Mountains. *Geol* 9(1):10-15. doi:10.1130/0091-7613(1981)9<10:PTOTAR>2.0.CO;2
- Krivoruchko K, Gribov A, Hoef JM (2006) A new method for handling the nugget effect in kriging, in Coburn TC, Yarus JM, Chambers RL, eds. *Stochastic modeling and geostatistics: Principles, methods, and case studies*. AAPG Comp Appl Geol 5:81-89
- Krivoruchko K (2012) Empirical Bayesian Kriging implemented in ArcGIS geostatistical analyst. *ESRI ArcUser* 2012:6-10
- Kulkarni RB (1984) Bayesian kriging in geotechnical problems, in A. Verly et al. 9eds.), *Geostatistics for Natural Resources Characterization*. D. Redidel, Amsterdam 775-786
- Link HL, Roberts MT (1986) Pennsylvanian paleogeography of the Ozarks, Arkoma, and Ouachita Basin in east-central Arkansas, sedimentary and igneous rocks of the Ouachita Mountains of Arkansas. *Ark Geol Comm CP(2):37-60*

- McEwaine (1966) The southern Club Rock slide of April 25. *Ark Geol Surv Cons Rep* 1
- McFarland JD, Stone CG (1981) A case history of a major landslide on Crowley's Ridge, Village Creek State Park, Arkansas. *Ark Geol Comm* MP18:45- 52
- McFarland JD (1992) Landslide features of Crowley's Ridge. *Ark Geol Comm* IC-31:1-30
- McFarland JD, Stone CG (1995) Hot Spring Dinging Landslide, Hot Springs, AR. *Ark Geol Comm*
- McFarland JD, Hanson D (2005) A major landslide of Greers Ferry Lake. *Ark Geol Comm*
- Nijkamp P (1980) *Environmental policy analysis: Operational methods and models*. Wiley, New York
- Omre H (1987) Bayesian kriging - Merging observations and qualified guesses in kriging. *Math Geol* 19(1):25-39. doi:10.1007/BF01275432
- Pontiff JL (2007) *Regional stratigraphic framework of Morrowan strata, northern Arkoma Basin*. Thesis, University of Arkansas
- Radbruch-Hall DH, Colton RB, Davies WE, Lucchitta I, Skipp BA, and Varnes DJ (1982) Landslide overview map of the conterminous United States. *US Geol Surv Open-file Rep* 97-289. <https://pubs.usgs.gov/pp/p1183/pp1183.html>. Accessed 10 April 2017
- Saaty TL (1977) A scaling method for priorities in hierarchical structures. *J Math Psych* 15(3):234-281. doi:10.1016/0022-2496(77)90033-5
- Saaty TL, Vargas LG (1991) *Prediction, projection, and forecasting: Applications of the analytic hierarchy process in economics, finance, politics, fames, and sports*. Boston, MA
- Salciarini D, Fanelli G, Tamagnini C (2017) A probabilistic model for rainfall-induced shallow landslide prediction at the regional scale. *Landslides* 1-16. doi:10.1007/s10346-017-0812-0
- Selby MJ (1980) A rock mass strength classification for geomorphic purposes: with tests from Antarctica and New Zealand. *Z Geomorph* 24:31-51
- Shahabi H, Hashim M (2015) Landslide susceptibility mapping using GIS-based Statistical models and remotes sensing data in tropical environment. *Sci Rep* 5(9899):1-15. doi:10.1038/srep09899
- Singhal BBS, Gupta RP (2010) *Applied hydrogeology of fractured rocks: 2nd Ed*. Springer, Drodrecht
- Tobler W (1970) A computer movie simulating urban growth in the Detroit region. *Econ Geogr* 46:234-240. doi:10.2307/143141
- United States Geological Survey (2000) *The geologic map of Arkansas, Digital version*. US Geol Surv <http://cpg.cr.usgs.gov/pub/other-maps.html>. Accessed 10 April 2017
- Varnes HD (1949) *Landslide problems of southwestern Colorado*. US Geol Surv Circ 81:1-18
- Voogd H (1983) *Multicriteria evaluation for urban and regional planning*. Pion, London.

- Wang RY, Strong D (1996) Beyond accuracy: What data quality means to data consumers. *J Manag Info Sys* 12(4):5-34
- Watts SG, Shankaranarayanan AE (2009) Data quality assessment in context: A cognitive perspective. *Decis Sup Sys* 48:202–211. doi:10.1016/j.dss.2009.07.012
- Zachry DL (1979) Early Pennsylvanian Braided Stream Sedimentation, Northwest Arkansas. *Tulsa Geol Soc Spec Pub No 1*
- Zachry DL, Sutherland KP (1984) Stratigraphy and depositional framework of the Atoka formation (Pennsylvanian) Arkoma Basin of Arkansas and Oklahoma. *Okla Geol Sur Bull* 136:9-17
- Zadeh LA (1965) Fuzzy sets. *Inf and control* 8(3):338-353. doi:10.1016/S0019-9958(65)90241-X
- Zadeh LA (1968) Fuzzy Algorithms. *Inf and control* 12(2):84-102. doi:10.1016/S0019-9958(68)90211-8

CHAPTER 3

Rowden and Aly *Geoenvironmental Disasters* (2018) 5:6
<https://doi.org/10.1186/s40677-018-0098-0>

GIS-BASED REGRESSION MODELING OF THE EXTREME WEATHER PATTERNS IN ARKANSAS, USA

Kyle W. Rowden and Mohamed H. Aly*

ABSTRACT

BACKGROUND

Investigating the extreme weather patterns (EWP) in Arkansas can help policy makers and the Arkansas Department of Emergency Management in establishing polices and making informed decisions regarding hazard mitigation. Previous studies have posed a question whether local topography and landcover control EWP in Arkansas. Therefore, the main aim of this study is to characterize factors influencing EWP in a Geographic Information System (GIS) and provide a statistically justifiable means for improving building codes and establishing public storm shelters in disaster-prone areas in the State of Arkansas. The extreme weather events including tornadoes, derechos, and hail that have occurred during 1955-2015 are considered in this study.

RESULTS

Our GIS-based regression analysis provides statistically robust indications that explanatory variables (elevation, topographic protection, landcover, time of day, month, and mobile homes) strongly influence EWP in Arkansas, with the caveat that hazardous weather frequency is congruent to magnitude.

CONCLUSIONS

Results indicate a crucial need for raising standards of building codes in high severity regions in Arkansas. Topography and landcover are directly influencing EWP, consequently they make future events a question of “when” not “where” they will reoccur.

KEYWORDS: Extreme Weather, GIS, Regression Modeling, Risk Assessment, Arkansas

INTRODUCTION

Arkansas is located in the Southcentral Heartland of the United States of America (Fig. 1) and ranks 4th and 5th in the USA for tornado-related fatalities and injuries, respectively. From 1955 to 2015, there have been 306 fatalities and over 4,800 injuries related to severe weather in Arkansas (FEMA 2008). Although no precise definition exists for what is colloquially referred to as “Tornado Alley”, the Federal Emergency Management Agency (FEMA) insets Arkansas in the center of the highest frequency region of the USA for high wind events (tornadoes and derechos), as shown in Figure 1. Hail, which can range in magnitude from pea-size to grapefruit size (NOAA 2017) has been considered with these wind events. Such geoenvironmental weather-related hazards will continue to reoccur, thus it is fundamental to investigate their spatial and temporal patterns to advance understanding of their reoccurrence and to minimize human and environmental vulnerability.

Spatio-temporal analysis of the extreme weather patterns (EWP) has been exhaustively conducted for other states (e.g. Bosart et al. 2006; Gaffin 2012; Lewellen 2012; Lyza and Knupp 2013); but until recently very limited analysis, focused on just storm severity of individual events and topography, has been conducted over Arkansas (e.g. Selvam et al. 2014; 2015; Ahmed and Selvam 2015a; 2015b; 2015c; Ahmed 2016). A three-dimensional overview of Arkansas’

topography and weather patterns related to predominant wind directions elucidates a preference for these prevailing winds to funnel hazardous weather into concentrated zones along the eastern front of the Ouachita and Boston Mountains as well as through the Arkansas River Valley (Fig. 2). Unfortunately, the severe weather tracks are mainly concentrated in the highest populated areas in Arkansas.

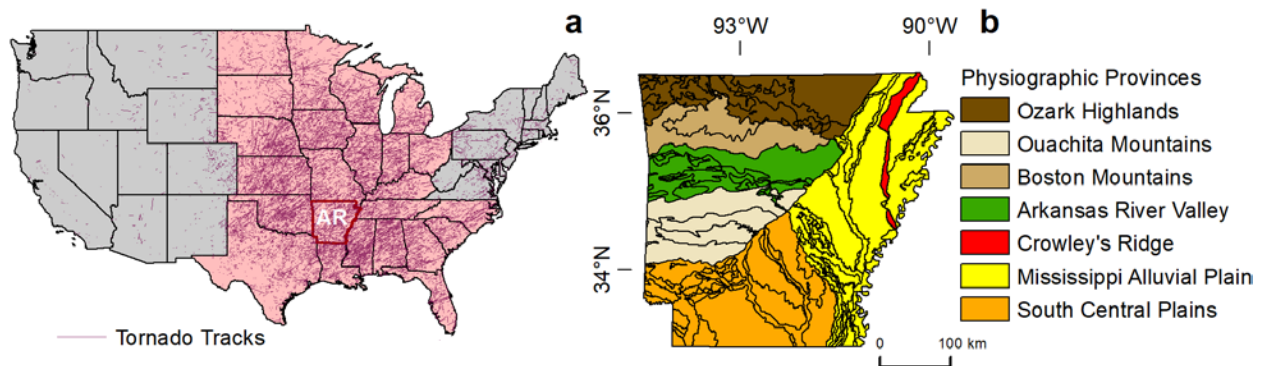


Fig. 1 a. Light red region indicates the highest frequency of tornadoes in the United States of America. AR denotes the State of Arkansas. b. Physiographic provinces of Arkansas that have topographic and land surface features influencing severe weather patterns

A common misconception propagates an axiom through rural communities that tornadoes do not occur in mountainous terrains, but this is just a myth (Lyza and Knupp 2013). Fujita (1971) first observed that tornadoes have a tendency to strengthen on the down-slope of their storm track. More researchers have followed Fujita’s footsteps pursuing the relationship between topography and severe weather events (e.g. LaPenta et al. 2005; Bosart et al. 2006; Frame and Markowski 2006; Markowski and Dotzek 2011; Gaffin 2012; Karstens et al. 2013; Lyza and Knupp 2013). Forbes et al. (1998) and Forbes (2001) provided more insightful observations: (1) widths of destructive swaths contract on down slopes, (2) intense swirls are most likely occurring at the base

of mountains or along the down slope path, (3) intensity of a tornado is likely to decrease on the upward slope, and (4) tornadoes are likely to weaken on a jump from one hill top to another and strengthen upon touching down on the adjacent hill. Lewellen (2012) elaborated on these observations and questioned whether topography might statistically provide zones of safety from severe weather. Other explanatory variables (EV) influencing damage include concentrations of mobile homes, often referred to as “trailer parks”. Keller and Niyogi (2013) examined the

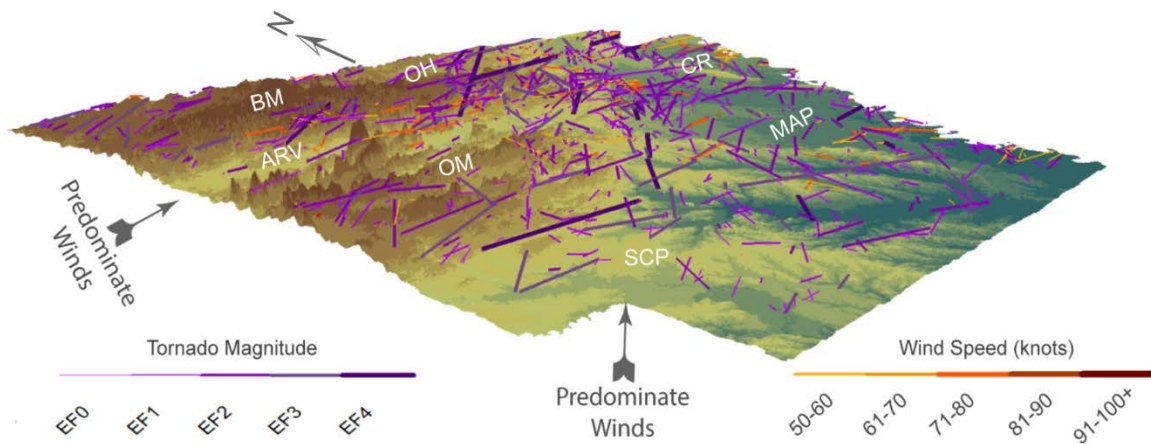


Fig. 2 Prevalent wind directions (southwesterly and westerly) and the related weather patterns. 1 knot = 1.852 km/hr (or 1 nautical mile/hr). Arkansas Physiographic provinces are indicated as: Ozark Highlands (OH), Ouachita Mountains (OM), Boston Mountains (BM), Arkansas River Valley (ARV), Crowley’s Ridge (CR), Mississippi Alluvial Plain (MAP), and South Central Plain (SCP)

phenomenon of tornado attraction to mobile home communities and determined that these communities do not attract strong weather events as much as these communities are constructed in the undesirable hinterlands that are heavily prone to severe weather patterns.

Severe weather will continue to strike Arkansas as well as the rest of the world. As this is unavoidable, then the main concern is how patterns of extreme weather can be used to promote effective disaster mitigation efforts. Crichton (1999) defines risk as the probability loss that may occur based on three components (Fig. 3): (1) hazards, (2) vulnerability, and (3) exposure. The specific objective of this study is to investigate spatial and temporal patterns associated with extreme weather phenomena (tornadoes, derechos, and hail) at the state level from 1955 to 2015 by standardizing and constraining all documented weather events to a 10x10-km grid. Grid standardization provides a systematic approach to examine subsets of severity, including frequency and magnitude, via extrapolating statistics related to fatalities, injuries, and property loss. Geostatistical analysis utilizing Ordinary Least Squares (OLS) regression is powerful in



Fig. 3 The risk hazard triangle (adapted from Crichton 1999). Hazards pose no risk if there is not some amount of exposure and vulnerability

determining the most disaster-prone areas in Arkansas, and results support initiatives to improve building codes in high risk areas (e.g. FEMA 2008; Safegaord 2009). This research will definitely improve awareness of potential hazards related to extreme weather and will help the policy makers in making informed decisions with regard to public storm shelters across Arkansas. Moreover, the

developed GIS procedure can be replicated to investigate the spatio-temporal patterns of severe weather in other locations across the world.

STUDY AREA

Along with tornadoes, Arkansas is prone to powerful supercell thunderstorms that can produce large magnitude hail storms and deadlier derechos (also known as “straight-line winds” or “micro-bursts”), which are strong wind events with gusts exceeding 50 knots. Historically, the highest injury and fatality counts related to severe weather in Arkansas and the rest of USA predate the 1950’s when the first weather forecasting station was installed at Tinker Air Force Base in Oklahoma, coinciding with President Harry Truman’s signing of the Civil Defense Act (CDA) in 1950 (Galway 1985; Bradford 1999;2001; Coleman et al. 2011). The CDA mandated installation of warning sirens across the USA, which became the saving grace for countless Americans from severe weather strikes.

Although the National Weather Service (NWS) issues weather forecasts, severe weather warnings come out of the local offices (located in Little Rock in the case of Arkansas) and the Storm Prediction Center (SPC) releases severe storm watches (Edwards 2017). Early detection and warning are important factors reducing exposure to severe weather, but still the contemporary technology cannot predict weather with 100% accuracy. The National Climatic Data Center (NCDC), part of the National Oceanic and Atmospheric Administration (NOAA), has recorded 1,681 tornadoes from 1955 to 2015 (NCDC 2013; NOAA 2017). Figure 4 tragically shows fatalities and injuries suffered by Arkansas during the time frames examined in this study.

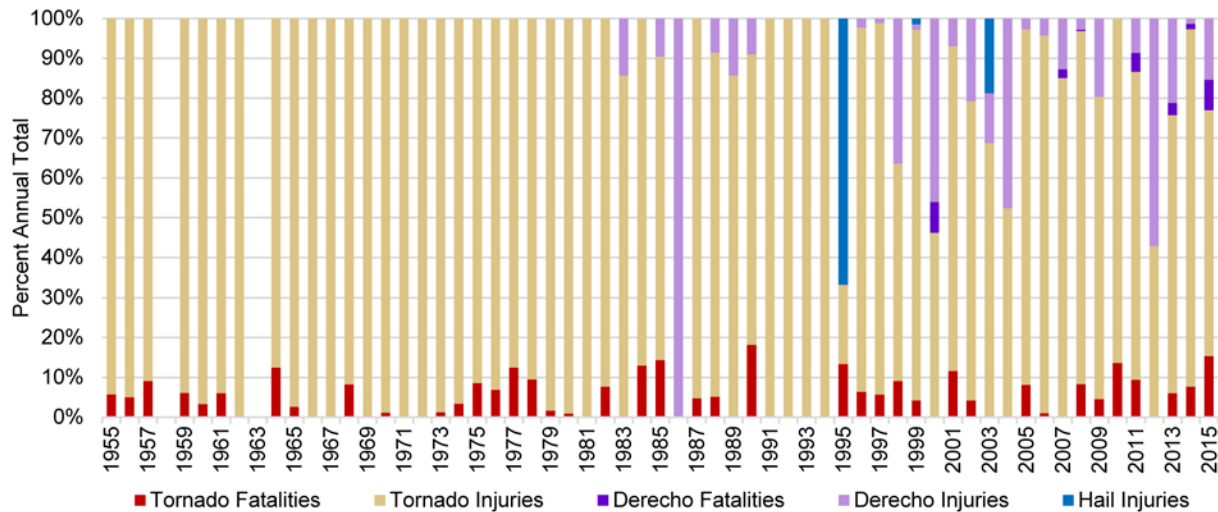


Fig. 4 Injuries and fatalities due to severe weather in Arkansas during 1955-2015. No fatalities have been attributed directly to hail. Property damage has exceeded \$660 million dollars. A total of 132 injuries and 15 fatalities are attributed to derechos, with 27 injuries and 11 deaths just between 2010 and 2015. Tornadoes are the most damaging events with 291 fatalities and 4,723 injuries along with billions of dollars in property damage during the study period. No fatalities or injuries occurred in years 1958 and 1963

Arkansas has three main population centers located in unique regions across the state. These being the Little Rock metropolitan area that includes Little Rock, Jacksonville, Cabot, Benton, Maumelle, and Conway located in the geographic center of the state; northwest Arkansas (NWA) which includes Fayetteville, Springdale, Rogers, and Bentonville; and lastly Jonesboro in northeastern Arkansas. All these regions are vital socio-economic hubs for the state and the USA and unfortunately are prone to the most violent episodes of hazardous weather.

The city of Little Rock (Pulaski County) houses the State Capital along with all major state agency headquarters as well as large private sector corporations such as Dillard's, a fortune 500 company headquartered in Little Rock (Fortune 2017). Little Rock's population is ~200,000 people. When taking into consideration the counties adjacent to Pulaski County, there are over 700,000 residents with even more working in this region daily (U.S. Census 2016). Central Arkansas is consistently hit with the highest frequency and magnitude events annually. For

instance, on April 27, 2014, the Mayflower Tornado touched down about 25 km northwest of Little Rock carving a 70-km path of destruction. This tornado remained on the ground for over 60 minutes, reaching a maximum width of ~1 km, killed 16 lives and injured over 120 people. This was the second deadliest single tornadic event in Arkansas in the past 50 years.

NWA is the second most populated area in the state with the two counties (Benton and Washington) having a combined total of 500,000 residents (U.S. Census 2016). The University of Arkansas located in Fayetteville is the largest university in the state with a current enrollment of ~28,000 students in fall of 2017 (UA 2017). Multiple fortune 500 companies are headquartered in NWA, these being Walmart (#1 biggest company in the world), Tyson Foods, J.B. Hunt Transportation (Fortune 2017) along with the ancillary business these companies drawn in. Walmart, and its related U.S. distribution, is anchored in Arkansas with 6 of Arkansas' 10 distribution centers, supporting the billion-dollar corporation being located in NWA. Although not immediately in Arkansas, the May 22, 2011, EF-5 Joplin Tornado was one of the most powerful and deadliest tornadoes in U.S. history and was responsible for 158 fatalities, over 1,150 injuries, and \$2.8 billion dollars' worth of damage (Kuligowski et al. 2014). It is conceivable that a tornado of this magnitude could strike NWA.

Lastly, Jonesboro, the county seat for Craighead County has a population of more than 100,000 residents and supports the second largest university in the state; Arkansas State University with 25,000+ enrollments (ASU website 2017). Although this region of Arkansas doesn't have the quantity of people as the aforementioned regions, Jonesboro serves as the agricultural center for Arkansas as well as much of the USA. Arkansas is the number-1 rice producing state in the USA by raising more than 50% of domestic rice. Billion dollars agriculture companies, such as Riceland

Foods, Inc., operate out of this region and export more than 60% of Arkansas rice (ARFB 2017) to the international market.

The Mississippi Alluvial Plain (MAP) often referred to as the Arkansas Delta is a flat lowland physiographic region nearly void of any topographic relief apart from Crowley's Ridge just west of Jonesboro. This type of landscape is particularly favorable for agriculture but meanwhile it is also proper for broad sweeping weather patterns with the capability of inundating the region with heavily rains. For instance, a hail event occurred in May 2015 in close proximity to Walnut Ridge (45 km northwest of Jonesboro) produced hail up to 5 inches in diameter. Hail of this size is large enough to kill people and livestock, as well as destroy roofs of houses. Fortunately, this event missed a direct hit on Walnut Ridge and occurred across the agricultural land adjacent to the town. Derechos frequently strike this region accounting for 30% of all derechos in the state. Single microburst can cause millions of dollars in damage such as the event on May 12 of 1990 that was responsible for \$6 million dollar in property loss. Derechos' magnitudes may exceed 100 knots, such as the recent event on January 22, 2012. This same weather system also spawned 7 tornadoes and blanketed the MAP region with hail up to 3 inches; emphasizing the interconnectedness of all three severe-weather types within a single storm. Event details and weather-related statistics are extracted from the GIS metadata that are publicly available through NOAA and NWS geodata as part of the Storm Prediction Center's Severe GIS (SVRGIS) data repository.

METHODOLOGY

GIS is employed to categorize and compartmentalize unique attributes from datasets into equal interval 10x10 km grids for the entire state. Grid analysis provides a higher level of specificity to weather patterns compared to the broad, low precision county level analysis previously conducted by multiple governmental and state agencies (e.g. FEMA 2002; 2008; NCDC 2013). The complete process along with the conducted regression analysis steps are demonstrated in the flowchart shown in figure 5 and are explained below.

GRIDDING AND STANDARDIZING INPUT DATA

Fishnetting allows storm tracts to be standardized into grids, supporting field summing, as well as later analysis of original attributes. Grid size is standardized to 10x10 km in this study. A 1-arc second digital elevation model (DEM) for the state is classified into ten classes using an interval of 82.66 m that closely mirrored a stretch classification method. These respective elevation attributes are then joined to the 10x10 km grid. Primary alchemy applied to this analysis revolves around the spatial join tool available in ArcGIS release 5.10.1 presenting two valuable options: (1) one-to-one, where a 1:1 ratio is maintained and the choice to sum totals is used to get sums of attributes for each respective cell and (2) one-to-many, which allows user selected attributes from a line, representing a storm track, intersecting multiple grid cell to be added. The one-to-many spatial join has been used in this study to model event frequencies for each respective weather hazard.

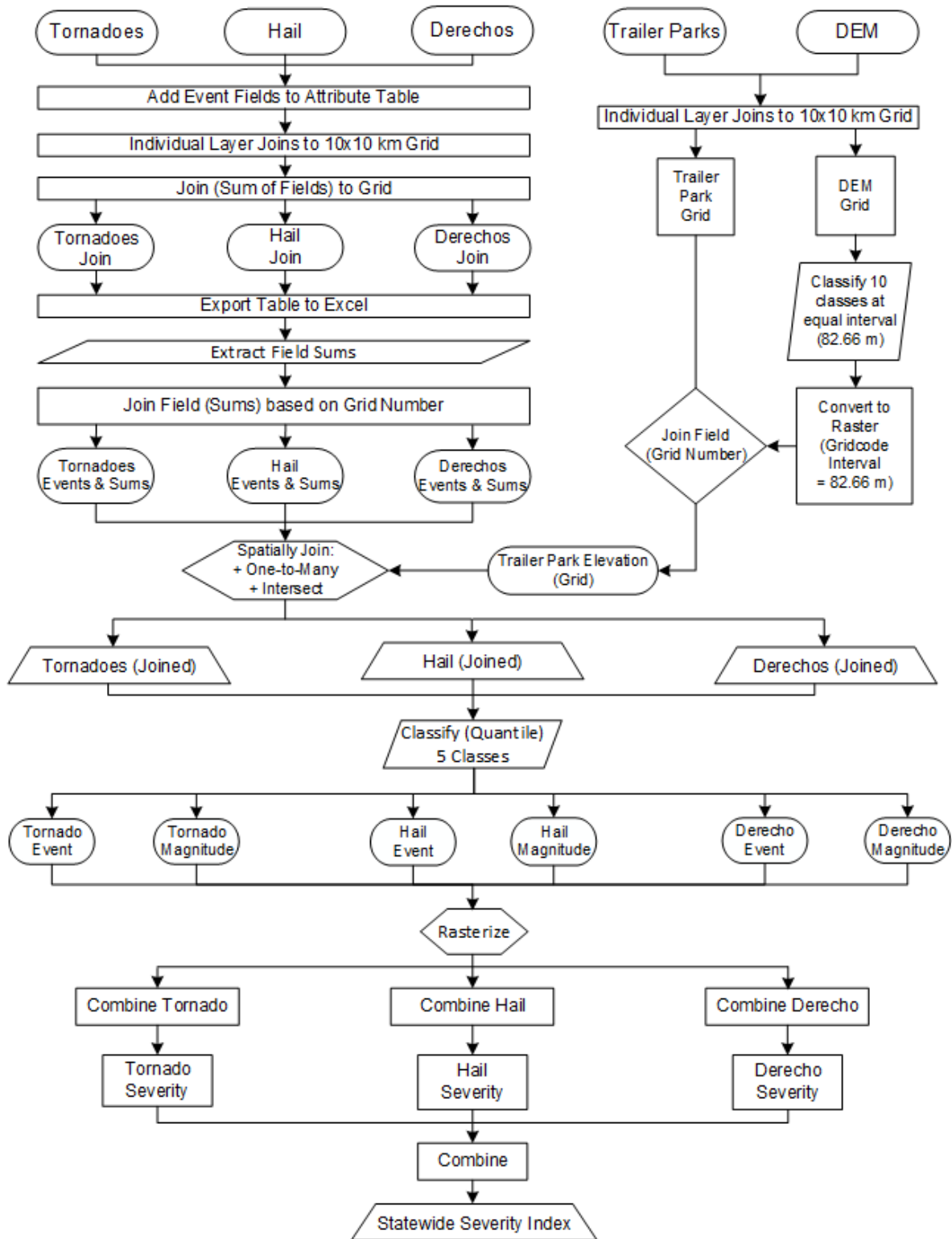


Fig. 5 Workflow for grid standardization and creating a statewide severity index

CREATING SEVERAL INDICES

Initially, event frequency and magnitude vectors are converted into raster, where the cell values of each respective variable become a grid code output, then the frequency and magnitude are combined for each weather event. Later, a severity index is established for each respective weather event, with each component of the triad being combined into a final statewide severity index using this simple formula:

$$SSI = TS * DS * HS \quad (1)$$

where *SSI* is the statewide severity index, *TS* is the tornado severity, *DS* is the derecho severity, and *HS* is the hail severity.

EXPLORATORY REGRESSION

Regression analyses provide a means for exploratory data trends, offering statistical scrutiny of influential spatio-patterns. The exploratory regression (ER) tool in ArcGIS (5.10.1) provides a simplistic means for trial and error experimentation, allowing the analyst to narrow down factors that may be influencing the dependent variable model. ER is employed in this study as a first step investigation to conduct an OLS regression on the most influential variables. Explanatory variables (EV) considered in this analysis are found to be: trailer parks, elevation, topographic protection, physiographic ecological sub regions. These variables are chosen based on results from previous works (e.g. LaPenta et al. 2005; Bosart et al. 2006; Frame and Markowski 2006; Markowski and Dotzek 2011; Gaffin 2012; Karstens et al. 2013; Lyza and Knupp 2013) that show strong correlations between topography, elevation, land cover features, and windward aspects of topographic features to directly influence strength and subsequent severity of weather events. Several statistical properties are used to determine the strength of EV.

The coefficient of determination referred to as *Adjusted R²* and evaluated by Steel and Torries (1960) as:

$$R_{adj}^2 = 1 - \left[\frac{\frac{SSE_{error}}{(n-k)}}{\frac{SST_{total}}{n-1}} \right] \quad (2)$$

where R is the coefficient for multiple regressions, k , denotes the quantity of coefficients implemented in the regression, n , the number of variables, SSE_{error} , the sum for standard error and SST_{total} is the total sum of squares.

The statistical *t-test* developed by Gosset (1908) can be simplified as:

$$t = \frac{z}{s} = \frac{(\bar{X} - \mu) \left(\frac{\sigma}{\sqrt{n}} \right)}{s} \quad (3)$$

where \bar{X} is representative of the sample's mean where the sample ranges from X_1, X_2, \dots, X_n , out of a size n , which follows a natural tendency of normal distribution between the variance in σ^2 and μ , with μ denoting mean population, and σ being the standard deviation in the population.

Koenker (BP) statistic that is a chi-squared test for heteroscedasticity, originally developed by Bruesch-Pagan (1979) and later adapted to by Koenker (1981), is expressed as:

$$LM = \frac{1}{2} \left[\frac{N}{n(N-n)} \right] \left[\sum_t^n \left(\frac{\hat{u}_t^2}{\hat{\sigma}^2} \right) - n \right]^2 \quad (4)$$

in which LM is a Lagrange Multiplier, N denotes the number of observations, n the sample size, \hat{u}_t^2 are the dependent gamma residuals, $\hat{\sigma}^2$ is the estimated residual variance in observations.

Akaike's Information Criterion correction (AICc) is used to estimate relative quality for a given statistical model and is based on information theory and serves as a means of ranking the quality of multiple to models with respect to one another. AICc is based on Akaike Information Criterion (AIC) (Akaike 1973; 1974; 2010) and corrects for a finite sample size:

$$AICc = AIC + \frac{2k(k+1)}{n-k-1} \quad (5)$$

with k denoting the number of parameters and n , the sample size (e.g. Burnham and Anderson 2002; Konishi and Kitagawa 2008).

The Jarque-Bera statistical test is used to check for data sample skewness and kurtosis match on a normal distribution curve through:

$$JB = \frac{n-k+1}{6} \left(S^2 + \frac{1}{4}(C - 3)^2 \right) \quad (6)$$

in which S is skewness in the dataset, C is the sample's kurtosis, n the number of observations, and k represents the quantity regressors (e.g. Jarque and Bera 1980; 1981; and 1987).

The reciprocal of tolerance (also known as the maximum Variance Inflation Factor - VIF) (Belsley et al. 1980; Belsley 1984; O'brien 2007) can be expressed as:

$$VIC = \left(\frac{1}{(1-R_i^2)} \right) \quad (7)$$

where tolerance of the i th variable is 1 less, the proportion of variance which is R_i^2 (O'brien 2007).

The Spatial Autocorrelation (SA) essentially draws on a Global Moran's I value based on Tobler's Law (1970) to calculate p-scores and z-scores. P-scores designate probability percentages that range from 0.10 to <0.01 (weak), null, and 0.10 to <0.01 (strong). Z-scores represent standard deviations, when combined with a strong corresponding p-scores indicate robust confidence. Ranges for Z-scores are (weak) <-2.58 up to (strong) >2.58. Moran's I is defined by ESRI (2016) as:

$$I = \frac{n \sum_{i=1}^n \sum_{j=1}^n W_{ij} z_i z_j}{S_0 \sum_{i=1}^n z_i^2}, \quad (8)$$

where deviation of an attribute's feature, I , from mean ($x_i - X$) is z_i , n denotes total feature count, spatial weighting between (i, j) becomes $W_{i,j}$, and lastly the amalgamation of these spatial weights is S_0 :

$$S_0 = \sum_{i=1}^n \sum_{j=1}^n W_{i,j}, \quad (9)$$

Z_I-scores are calculated with:

$$z_I = \frac{I - E[I]}{\sqrt{V[I]}}, \quad (10)$$

where:

$$E[I] = -\frac{1}{n-1}, \quad (11)$$

$$V[I]a = E[I^2] - E[I]^2, \quad (12)$$

ORDINARY LEAST SQUARES

OLS is perhaps the most commonly used form of regression analysis in GIS. Amemiya (1985) defines it as:

$$y = \beta_0 + \beta_1 X_1 + \beta_2 X_2 + \beta_3 X_3 + \dots \dots \beta_n X_n + \epsilon \quad (13)$$

where y is the dependent variable which is the variable that is predicting or explaining the model and is a function of X, which are coefficients representing EVs that, together, help answer y. β are regression coefficients that are calculated through algorithms running in the GIS background and β_0 is the regression intercept and represents an expected outcome for y and ϵ are the residual random error terms.

As part of the OLS process, we run a SA utilizing Global Moran's I, which determines the likeliness of randomly chosen EVs relative to their spatial distribution and impact. Other statistical outputs included in the final OLS include: (1) *StdError* and (2) *Robust_{SE}*, which are errors in standard deviation; (3) *t-statistic* and (4) *Robust_t* which are ratios between an estimated value of a parameter and a hypothesized value relative to standard error; (5) probability and (6) *robust probability (Pr)*, which are the statistically significant coefficients (p<0.01); should initial

probability values possess a significant (7) *Koenker* statistic, then (*pr*) is used to determine significance of coefficient; (8) *VIF* factors (>7.5) that are indicative of redundancy; (9) *Joint Wald* statistic, which help determine model's overall significance if *Koenker* value is significant; and finally (10) *AICc* and (11) R^2 , which are measures of model's overall fit and performance.

QUANTILE CLASSIFICATION

Quantile classification is used for the symbology of all choropleth maps. Quantile is chosen as the appropriate means for classification because it creates classes based on equal division of units in each class (e.g. Cromley 1996; Brewer and Pickle 2002; Burnham and Anderson 2002; Xiao et al. 2007, Sun et al. 2015). Quantile classification most closely represents the input data trends that are poorly represented using other classification methods, such as Jenks-Natural breaks, equal interval, standard deviation, and geometric classifications.

RESULTS AND DISCUSSION

Patterns with strong positive correlations are detected between the frequency of severe weather events and time of day, elevation, and magnitude (Tables 1-3). Primary patterns are explored in the preliminary determination of EV used in the exploratory regression. The three types of hazards showed a strong tendency to occur between 2:00 and 10:00 pm (Tables 1-3). This is a noteworthy observation because Arkansas becomes dark around 5:30 pm in fall and winter months, reducing the visual line-of-sight to nearly null and limiting rural residents visual warning detection. A second pattern is found at the elevation of 165 m with the highest frequency of 660 out of 1677 tornadic events (~40%) occurred during the study period. A higher frequency of hail and derecho events are found to occur at the 165-m elevation. A tertiary pattern is found occurring within a narrow range between 200 m and 250 m. A third pattern and the strongest positive correlation is found between frequency and magnitude, indicating a natural tendency for these weather hazards

to be strong in areas of high frequency. Such areas are experiencing the highest severity and risk. A fourth pattern found is that the spatial distribution of these events occurs in the central part of Arkansas in the surrounding area of Little Rock (Figures 2 and 12). This metropolitan area has the highest population density, ~350,000 residents – this number approaches 500,000 during work days. The highest severity rankings for all weather events are centralized around Little Rock. This area also has the highest property and crop damage due to extreme weather events.

Tornadoes are, by far, the most destructive and deadliest of the three weather types considered in this research (Fig. 4). Tornadoes have posed a serious risk for Arkansans long before weather data archival began in 1950. Figure 6 highlights several geospatial patterns and illuminates the directional tendency of tornado paths to propagate in a northeastern direction. Lineaments of destruction can be followed along the eastern flanks of the Ouachita and Boston Mountains (these physiographic features are marked in Fig. 1 and Fig. 2), with property damage totaling over \$300 million dollars in individual grid cells (Fig 6e). Crop damage is the least concern with respect to tornadoes. This being said, the majority of the highest magnitude EF-4 tornadoes has occurred in the past decade, including the April 27 of 2014 Mayflower tornado that killed 15 people and injured over 100 (Selvam et al. 2014). OLS analysis provides strong indications that the EV of month, time of day (TIME_ADJ), physiographic region (AR_ECO_ID), trailer parks, and topographic protection to be robust indicators in the final model, where * denotes statistical significant p-values in Table 1. OLS output has ± 2 standard deviations of residuals from best prediction indicating that EVs predict ~80% of the model as determined from residual R^2 value of 0.78686. Std output shown in figure 7 displays a dominant ± 1 std for over-prediction/under-prediction of the final model. These results are reliable being within the accepted ± 2 std of error.

Table 1 Ordinary Least Squares results for tornadoes

	Variable	Coefficient	StdError	t-Statistic	Probability	Robust_SE	Robust_t	Robust_Pr	VIF
Event	Intercept	2.9560	0.2807	10.5299	0.000000*	0.2917	10.1329	0.000000*	-----
	Month	0.0279	0.0059	4.7338	0.000003*	0.0058	4.8383	0.000002*	1.0391
	ADJ_TIME	0.0246	0.0035	7.0107	0.000000*	0.0031	7.8801	0.000000*	1.1056
	SUM_MAG	0.4708	0.0042	112.0444	0.000000*	0.0049	96.6009	0.000000*	1.1092
	AR_ECO_ID	-0.0021	0.0002	-13.1645	0.000000*	0.0002	-11.4925	0.000000*	1.0497
	Protection	0.1328	0.0517	2.5702	0.010193*	0.0403	3.2951	0.001009*	1.0600
Magnitude	Intercept	-6.3259	0.5174	-12.2254	0.000000*	0.4869	-12.9926	0.000000*	-----
	Month	-0.0274	0.0109	-2.5071	0.012203*	0.0107	-2.5624	0.010423*	1.0452
	ADJ_TIME	0.0096	0.0065	1.4702	0.141599	0.0057	1.6650	0.096012	1.1194
	Event (Sum)	1.6066	0.0145	111.0131	0.000000*	0.0173	92.6609	0.000000*	1.1401
	Elevation	-0.0011	0.0004	-3.0899	0.002030*	0.0004	-3.0349	0.002434*	1.9239
	Trailer Parks	-0.0411	0.0080	-5.1587	0.000001*	0.0082	-5.0265	0.000001*	1.1378
	AR_ECO_ID	0.0054	0.0004	15.1201	0.000000*	0.0004	13.6639	0.000000*	1.5146
	Protection	0.0552	0.1118	0.4935	0.621665	0.0894	0.6170	0.537257	1.4571
			Joint Wald	Jarque-Bera	Koenker (BP) Statistic	AICc	Adjusted R2		
			11822.594	254.1233	1002.2988	13317.7251	0.78686		

Significant p-values ($p < 0.01$) are denoted by *, *StdError* is the standard deviation error, *t-statistic* is the ratio between estimated and hypothesized values relative to *StdError*, probability and *robust probability* (p_r) are significant when ($p < 0.01$), *Koenker* statistic determines significance of coefficients, and *VIF* is the variance inflation factor with values >7.5 are indicative of redundancy. *Joint Wald* determines overall significance if *Koenker* value is significant, *AICc* and R^2 represent overall fit and performance

Lyza and Knupp (2013) noted four common modes of behavior with tornadoes that can help explain the high magnitude and frequency in central Arkansas along with the protected zones in the Ouachita and Boston Mountain region immediately north of the Arkansas River Valley. Mode 1: where tornadic strength deteriorates on the up slopes, proved to be consistent in the findings of Selvam et al. (2014) with the Mayflower Tornado. Mode 2: tornado whirl pattern

intensifies on plateaus but weakens as the whirl moves off the plateau, potentially helping to explain the central Boston Mountain low severity zone. Mode 3: tornado tracts tend to follow valleys like

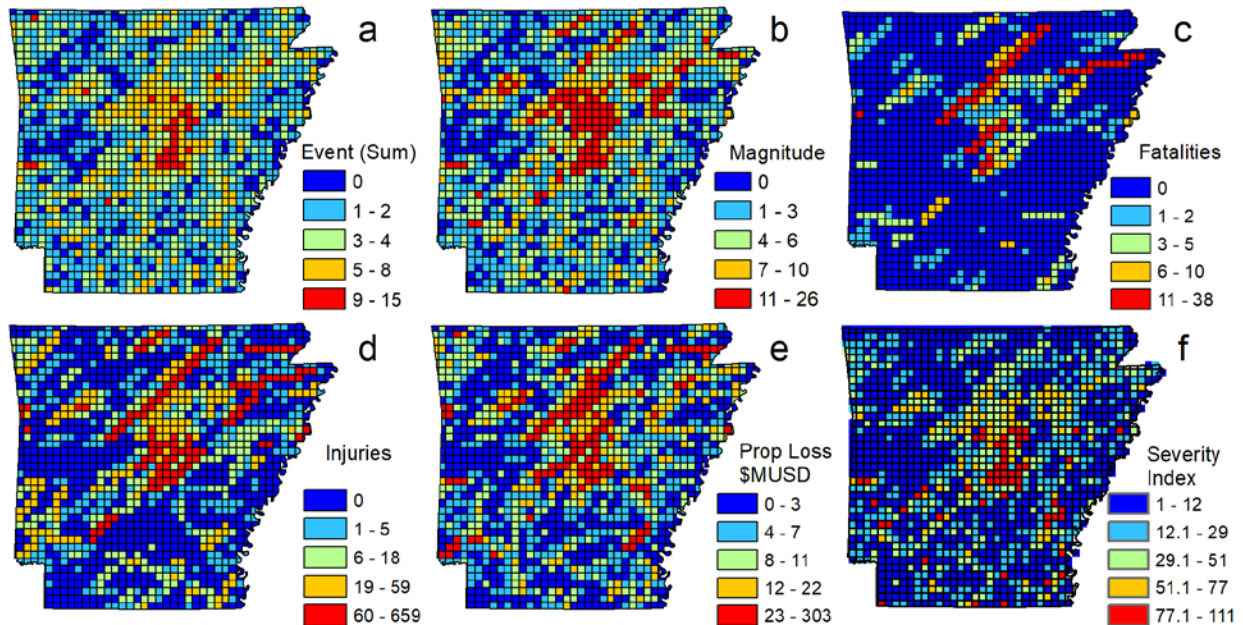


Fig. 6 Tornado Damage (grid cell = 10x10 km): a. Sum of all events (frequency) b. Sum of EF tornado magnitudes c. Fatalities (some grids approach 40 fatalities over the 60-yr study period) d. Injuries (many grids show 650+ injuries over the study period) e. Property damage follows the same path of the largest magnitude tornadic events f. Tornado severity index

a hallway, once again related to the Ouachita Mountains which are systematically folded long linear ridges and valleys helping funnel wind driven weather patterns from west to east into Little Rock. Mode 4: tornadoes have a tendency to trace the edges of ridges and plateaus. That has been also observed by Selvam et al. (2014) in Mayflower and can explain the strong tendency of EF-3 and EF-4 tornadoes to trend along the eastern boundary that the Ouachita Mountains makes with the Mississippi Embayment (refer back to Fig.1 for physiographic provinces of Arkansas).

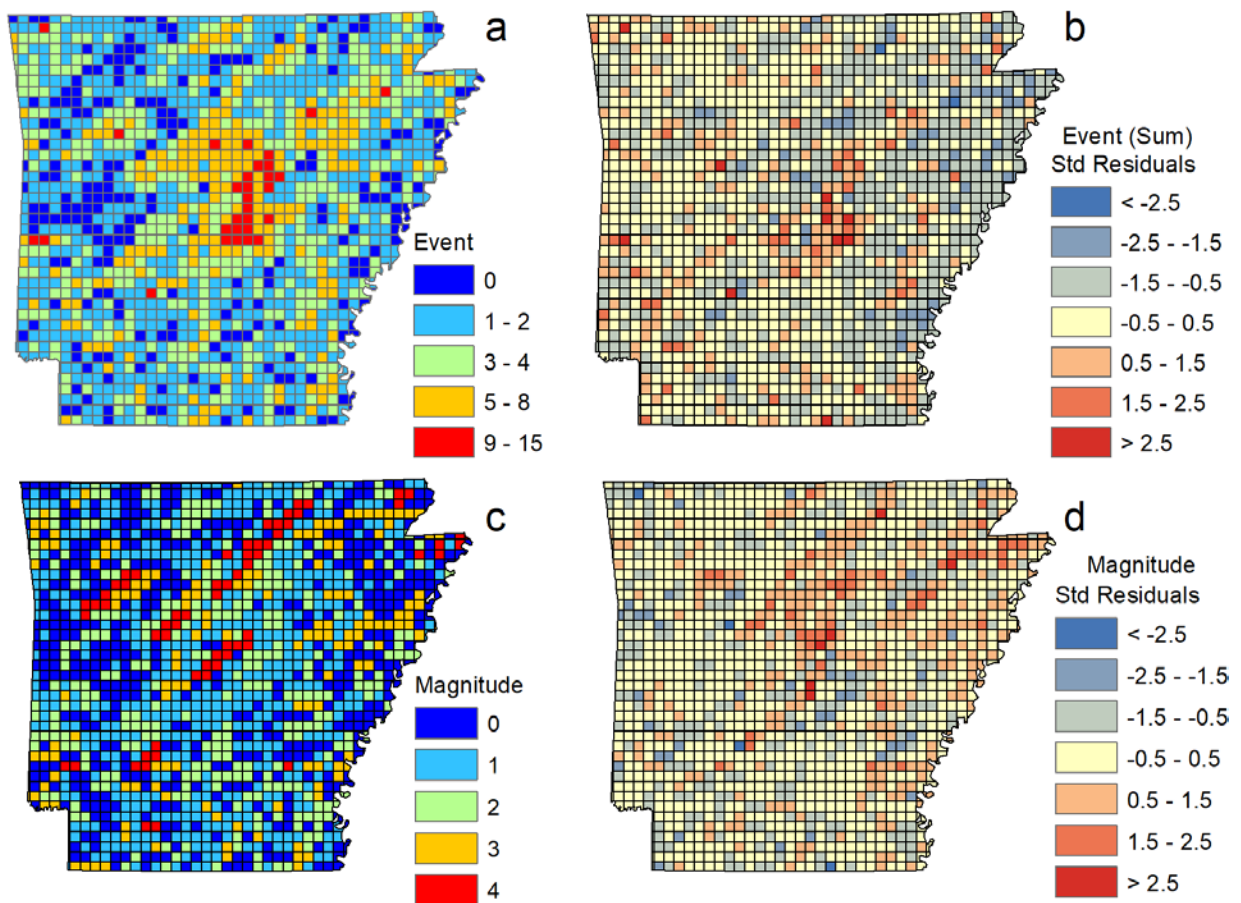


Fig. 7 Ordinary Least Squares regression analysis for explanatory variables [month, time of day (TIME_ADJ), physiographic region (AR_ECO_ID), trailer parks] influencing frequency and magnitude of Tornadoic Events. Grid cell = 10x10 km

Derechos are the second most destructive hazardous weather events in Arkansas. Investigation of spatial patterns has identified the highest magnitude cluster in northwest Arkansas. This is critical because NWA has the second highest population in the state, 300,000+ residents as well as a large commuter group working in the metropolitan area, and the region is an economic hub for the USA. Property damage and crop loss may reach into \$17.4 million dollars for single grid cells (Fig. 8). Fatalities are infrequent but do occur with these events, however injuries are more common (Fig. 4) due to the violent nature (50-100 knots) and the abruptness of these events, which just seem to come out of nowhere. OLS conducted on derecho events and magnitude (Fig.

9), using EVs of time, month, elevation, topographic protection, sum of magnitudes, sum of events, mobile home concentration, and eco-region, has produced robust and statistically significant ($p < 0.01$) coefficients, except for elevation, which is not found to be a good EV for event frequency although patterns are observed at specific elevations previously mentioned. Outside of these tight elevation windows, random patterns are observed. Table 2 shows the OLS outputs for the regression analysis. The R^2 of 0.9857 has a strong indication that the EVs chosen are sufficient at explaining the dependent variables. OLS shows that all explanatory inputs have VIF values below 2, where VIF values > 7.5 indicate redundancy of EVs.

Table 2 Ordinary Least Square results for derechos

	Variable	Coefficient	StdError	t-Statistic	Probability	Robust_SE	Robust_t	Robust_Pr	VIF
Event	Intercept	-32.346	2.3571	-13.7229	0.000000*	1.9912	-16.2441	0.000000*	-----
	Elevation	0.001	0.0016	0.6341	0.5260	0.0013	0.7589	0.4479	1.7764
	Month	0.407	0.0650	6.2605	0.000000*	0.0620	6.5668	0.000000*	1.0309
	TIME_ADJ	0.128	0.0258	4.9677	0.000001*	0.0248	5.1690	0.000001*	1.0270
	AR_ECO_ID	0.024	0.0016	15.1470	0.000000*	0.0015	15.3767	0.000000*	1.3115
	Protection	4.716	0.4971	9.4886	0.000000*	0.3091	15.2565	0.000000*	1.4236
Magnitude	Intercept	-423.667	41.0222	-10.3278	0.000000*	33.5516	-12.6273	0.000000*	-----
	Trailer Parks	2.423	0.5258	4.6078	0.000006*	0.5302	4.5697	0.000007*	1.1736
	Event (Sum)	39.873	0.1577	252.7619	0.000000*	0.1959	203.5371	0.000000*	1.1379
	Elevation	-0.425	0.0281	-15.1447	0.000000*	0.0255	-16.6968	0.000000*	1.8430
	Month	4.531	1.1255	4.0255	0.000065*	1.0887	4.1618	0.000037*	1.0340
	TIME_ADJ	1.603	0.4466	3.5889	0.000348*	0.4341	3.6920	0.000237*	1.0294
	AR_ECO_ID	0.340	0.0284	11.9668	0.000000*	0.0272	12.5045	0.000000*	1.4518
	Protection	61.355	8.6204	7.1175	0.000000*	6.3061	9.7296	0.000000*	1.4340
			Joint Wald	Jarque-Bera	Koenker (BP) Statistic	AICc	Adjusted R2		
			409245.6	5144.80	3643.4876	74204.573	0.9857		

Results are initially derived from exploratory regression analysis of explanatory variables to determine variables that have had the most significant influence

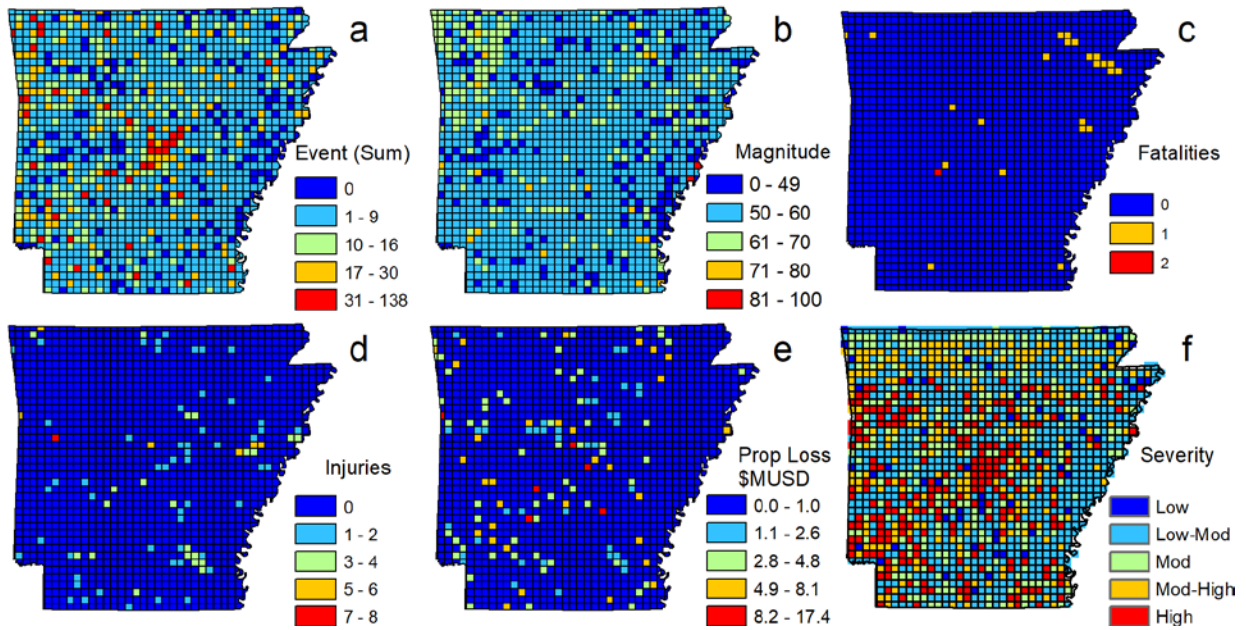


Fig. 8 Derecho damage (grid cell = 10x10 km): a. Sum of all events b. Derecho magnitude (0-100 knots) c. Fatalities d. Injuries e. Property damage (structures or vehicles) f. Derecho severity index

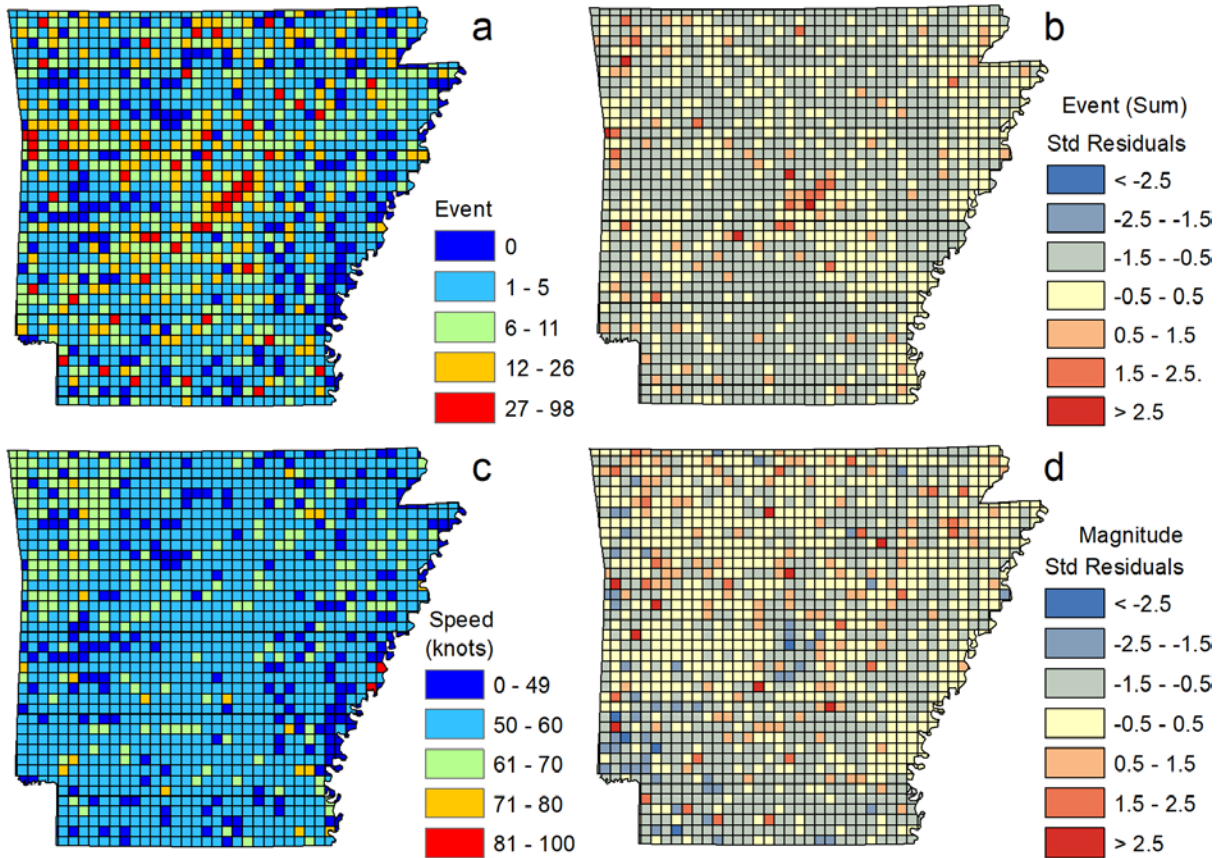


Fig. 9

Ordinary Least Squares regression analysis for explanatory variables influencing frequency and magnitude of derechos (grid cell = 10x10 km). OLS analysis of key explanatory variables showed to predict 98% of weather patterns for derechos with standard deviation (std) of residuals falling within ± 1 std

Hail is found to be the least destructive and the least problematic of the three weather types being considered in Arkansas. Hail is often associated with tornadoes and derechos but has occurred in localized incidents across the state, as shown in figure 10. A line of destruction amounting to \$7 million dollars' worth of crop loss and \$85 million dollars in property damage can be traced directly east of Little Rock, Arkansas (Fig. 10e). No fatality due to hail events has occurred during the study period and injuries are minimal (Fig. 4). Figure 10 displays OLS results

for event frequency and magnitude from inputs of EVs: time, month, elevation, topographic protection, sum of magnitudes, sum of events, eco-region. These EVs produced statistically significant coefficients with p-values <0.01, implying a robust model for explanation of historical hail patterns. OLS outputs in Table 3 provide ancillary validation for R^2 values of 0.84911, indicating the respective EVs chosen are sufficient at explaining ~85% of dependent variables. Applying EVs (time, month, elevation, topographic protection, sum of magnitudes, sum of events, concentration of mobile homes) to OLS regression analysis for events and magnitude (Fig. 11) shows that these EVs perform well at explaining most of the events but as with tornadoes and derechos still struggled at fully explaining the highest frequency and magnitude of events found in central Arkansas. This being said, even the outliers fall within ± 2 stds of error.

Our summed statewide severity product (Fig. 12) is consistent with local outputs from previous case studies by ADEM and FEMA (FEMA 2002) and clearly identifies various zones of severity across the entire state. This can help the state and other governmental agencies focus on the identified vulnerable spots to build public shelters and offer residential shelter grants. An interesting pattern of low severity found in the central Ouachita and Boston Mountains is consistent with topographic terrain protection theories proposed by previous researchers

The summed severity map shows a strong correlation between high severity and major population centers. A similar observation has been documented by Kellner and Niyogi (2013) where they spatially calculated touchdown points in Indiana to find that 61% of EF0-EF5 tornadoes touchdown within 1-3 km of urban landuse area bordering landcover classified as forest. Areas surrounding Little Rock in central Arkansas, which have had the highest incidence of tornadic and derecho activity, suffer from not only topographic terrain influence in the

Ouachita Mountains to the immediate west, but also a wind corridor effect through the Arkansas River Valley, as well as flat topography with land surface heterogeneity.

Table 3 Ordinary Least Squares results for hail

	Variable	Coefficient	StdError	t-Statistic	Probability	Robust_SE	Robust_t	Robust_Pr	VIF
Event	Intercept	-0.0296	0.2200	-0.1346	0.8929	0.2050	-0.1444	0.8852	-----
	SUM_MAG	0.8729	0.0009	1023.3266	0.000000*	0.0016	561.5929	0.000000*	1.0212
	MO	0.0409	0.0076	5.3547	0.000000*	0.0078	5.2433	0.000000*	1.0241
	HAIL_TIM_2	-0.0082	0.0033	-2.4808	0.013107*	0.0033	-2.4926	0.012680*	1.0196
	ELEVATION	0.0015	0.0001	10.8536	0.000000*	0.0001	12.5462	0.000000*	1.2704
	AR_ECO_ID	-0.0004	0.0002	-2.1620	0.030620*	0.0002	-2.2770	0.022785*	1.2861
Magnitude	Intercept	-0.2115	0.2501	-0.8456	0.3978	0.2248	-0.9406	0.3469	-----
	SUM_EVENT	1.1281	0.0011	1023.3266	0.000000*	0.0021	533.7691	0.000000*	1.0215
	MO	-0.0422	0.0087	-4.8542	0.000002*	0.0088	-4.7753	0.000003*	1.0244
	HAIL_TIM_2	0.0115	0.0037	3.0678	0.002173*	0.0037	3.0856	0.002049*	1.0194
	ELEVATION	-0.0018	0.0002	-11.2164	0.000000*	0.0001	-12.8938	0.000000*	1.2698
	AR_ECO_ID	0.0008	0.0002	4.1671	0.000037*	0.0002	4.5625	0.000007*	1.2851
			Joint Wald	Jarque-Bera	Koenker (BP) Statistic	AICc	Adjusted R2		
			47365.25	2445.7748	1057.0264	190276.91	0.84911		

OLS analysis shows very low VIF values meaning low model redundancy and all explanatory variables prove to be statistically significant denoted by asterisk (e.g. Fujita 1979; Lapenta et al. 2005; Bosart et al. 2006; Gaffin 2012; Lewellen 2012; Lyza and Knupp 2013). These observed patterns are consistent with aforementioned explanations for transitional zones of moderate severity as well as pockets of highest severity where topographic corridors funnel westerly storms along the eastern front of the Ouachita's and the second pattern through the Arkansas River Valley toward Little Rock.

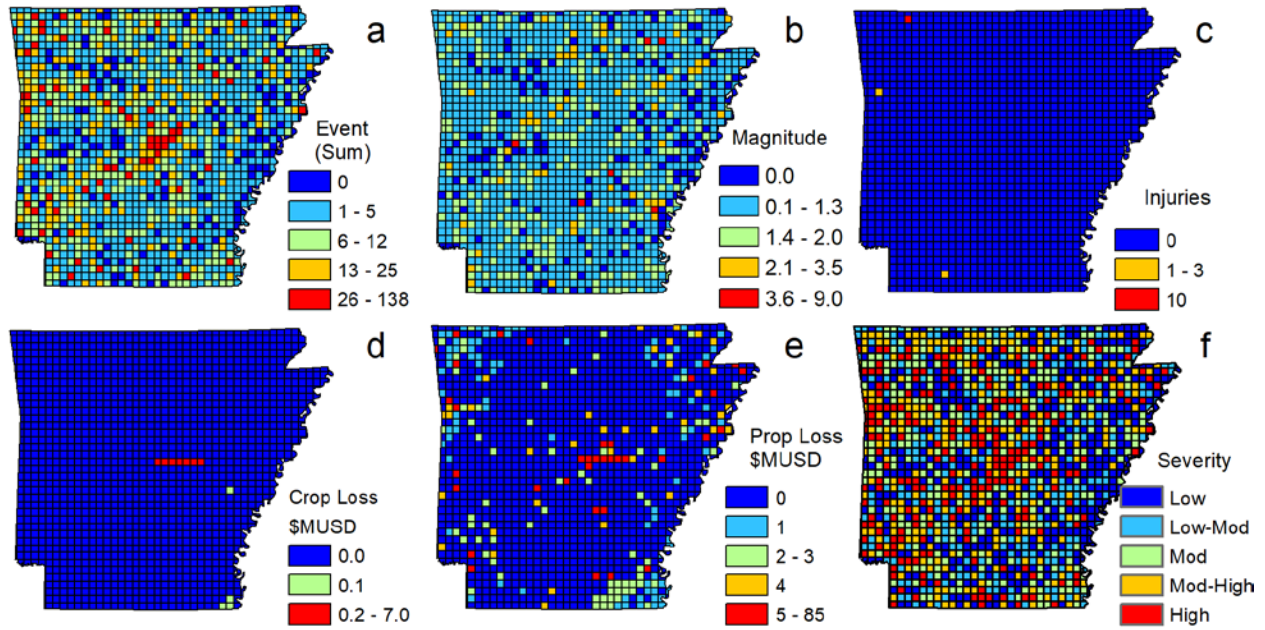


Fig. 10 Hail Damage (grid cell = 10x10 km): a. Sum of all events b. Magnitudes for hail ranging between 0.1 and 9.0 (pea-size to grapefruit respectively) c. Fatalities d. Injuries sustained during hail events e. Property losses including structures and vehicles f. Hail severity index. No fatalities have been directly attributed to hail during the study period, so choropleth has been omitted and instead crop loss has been represented instead because of the significant damage

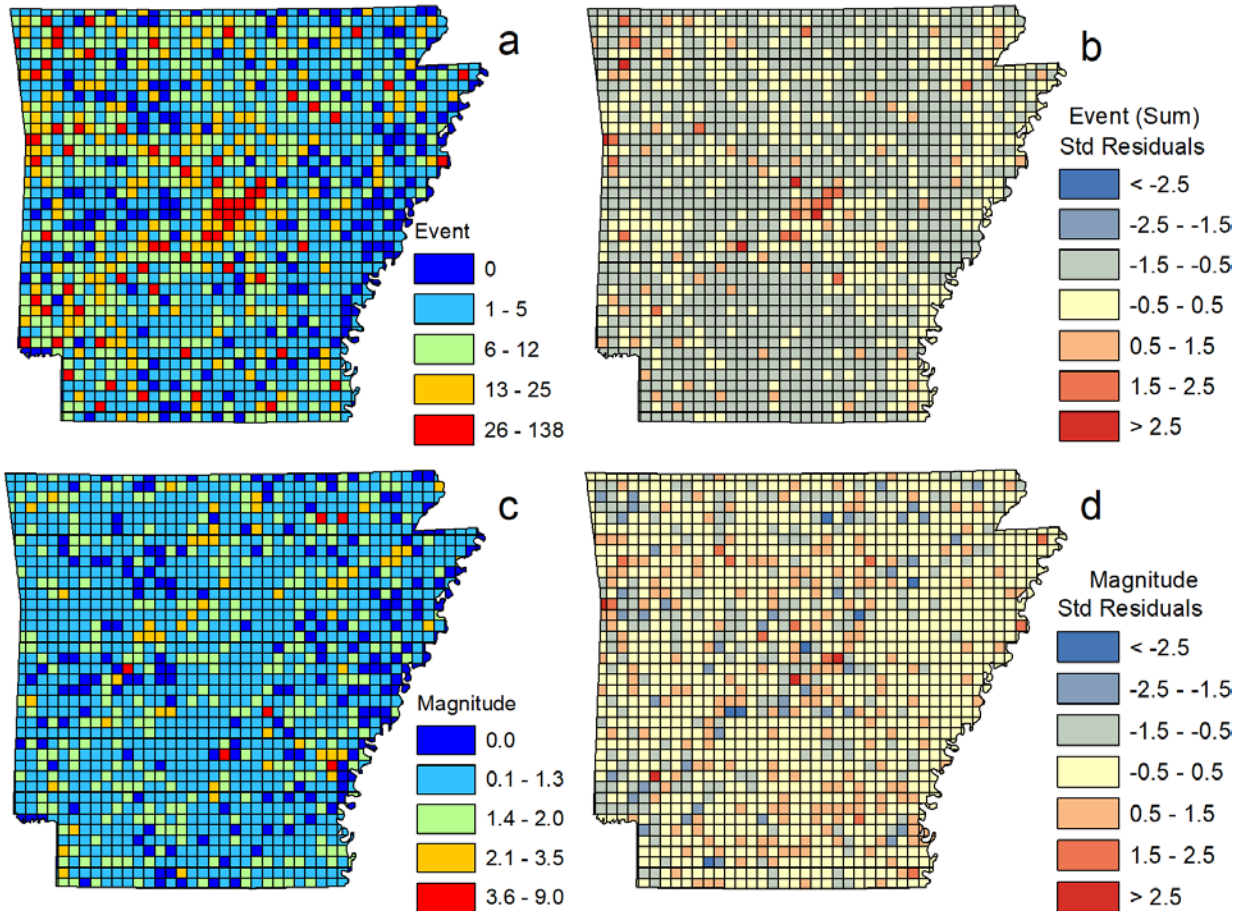


Fig. 11 Ordinary Least Squares regression analysis for explanatory variables influencing hail: a. frequency b. OLS are dominant within 1 standard deviation (std) for explanatory variable residuals c. magnitude d. OLS shows low (<1) standard deviation for residuals signifying robustness of model prediction

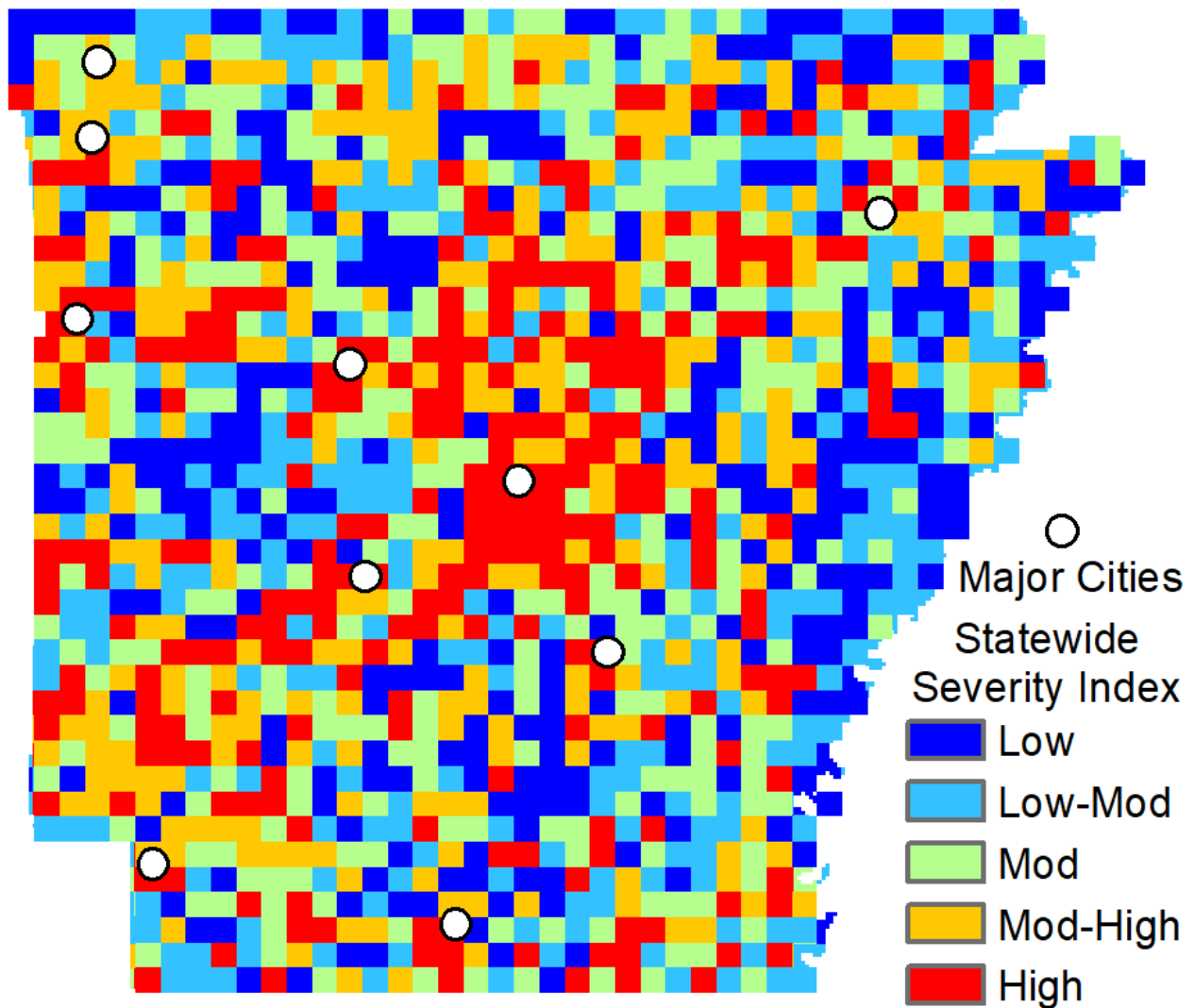


Fig. 12 Summed statewide severity index. Pattern indicates the natural tendency of hazardous weather to affect the central portion of Arkansas and shows protected zones across the state. Each grid cell equals 10x10 km

CONCLUSIONS

Complacency is a deadly human tendency that overcomes residents, especially when weather-related disasters have not occurred in recent years. Severe weather events sometimes occur simultaneously during the largest and most powerful storm system such as the example of the January 22 of 2012 that impacted the entire Arkansas Delta. Robust and viable statistics can help re-enforce the imperative need for storm shelters and higher building codes to better prepare

for such extreme weather events. Better understanding of severe weather patterns and preferential tendency for storms to frequent certain cities, regions, or trajectories is the first step in mitigating risk by minimizing exposure and vulnerability in these highest severity regions.

Analysis of the severe weather events from 1955-2015 reveals a very strong positive correlation with time of the day, in association with the three weather types under consideration. The extreme weather events are found to most likely occur between 2:00 and 10:00 pm local time. This is of vital importance because line-of-sight is reduced to near zero visibility at night, thus residents in most of fall and winter months must rely on National Weather Service warnings. Raising public awareness to the frequency and likelihood of such geoenvironmental risks occurring in evening hours may help bolster residents taking advantage of FEMA funding for building residential shelters in rural areas and community shelters in more urban settings.

Our findings in this study provide statistically robust evidence for variables that respond to Lewellen's (2012) question regarding whether it is statistically possible to prove that topography might influence regional weather patterns. Along with topographic influence, this study also found that other physiographic features such as elevation, physiographic provincial sub regions, and most importantly the windward protection afforded to leeward sides of physiographic features are statistically significant EV in predicting severe weather patterns.

The explanatory variables of time of day, month, elevation, physiographic region (subclass), topographic protection, elevation, and concentration of trailer parks are not only effective at forecasting severe weather patterns but also have been found to be statistically robust through OLS regression analysis. Susceptibility models based on these variables may provide substantially higher precision for spatio-temporal patterns, which in turn can be used by ADEM and FEMA as well as other first responding agencies, and residents to better access risk beyond

the broad umbrella of previous county-wide assessments. The developed methodology can be applied to a broad spectrum of severe weather around the globe to improve hazard mitigation and help with preparedness for geoenvironmental disasters.

DECLARATIONS

AVAILABILITY OF DATA AND MATERIAL

All weather and mobile home concentration data are publicly available from NOAA/NWS Geodata as part of the Storm Prediction Center's SVRGIS. Arkansas GIS data are publicly available from www.spc.noaa.gov/gis/svrgis/ and <https://gis.arkansas.gov>.

COMPETING INTERESTS

Both authors declare that they have no competing interests.

FUNDING

NASA EPSCoR RID grant #24203116UAF.

AUTHOR'S CONTRIBUTIONS

KR acquired the necessary data and conducted the GIS analysis and modeling with help and guidance from MA. Both authors developed the research idea and wrote the manuscript.

ACKNOWLEDGEMENTS

This study has been funded by the NASA EPSCoR program (grant #24203116UAF) and has been conducted using research facilities in the InSAR Lab which is part of the Center for Advanced Spatial Technologies – CAST at the University of Arkansas

REFERENCES

- Ahmed N, Selvam RP (2015a) Tornado-Hill interaction: damage and sheltering observations. *Inter. J. App. Earth Observ. and Geoinfo. Str.*
- Ahmed N, Selvam RP (2015b) Topography effects on tornado path deviation. University of Arkansas Computer Mechanics Lab Internal Paper, 1-31.
- Ahmed N, Selvam RP (2015c). Ridge effects on tornado path deviation. *Int. J. Civil Str. Eng. Res.*, 3(1):273-294.
- Ahmed N, Selvam RP (2016) Field observations and computer modeling of tornado-terrain interaction and its effects on tornado damage and path. Thesis, University of Arkansas.
- Akaike H (1973) Information theory and an extension of the maximum likelihood principle, in Petrov, B.N.; Csáki, F., 2nd International Symposium on Information Theory, Tsahkadsor, Armenia, USSR, September 2-8, 1971, Budapest. Akadémiai Kiadó, 267–281.
- Akaike H (1974) A new look at the statistical model identification. *IEEE Transactions on Automatic Control*, 19(6):716–723, doi:10.1109/TAC.1974.1100705.
- Akaike H (2011) Akaike’s Information Criterion. *Int. Encyc. Stat. Sci.* 2:1-25, doi:10.1007/978-3-642-04898-2_110.
- Arkansas Farm Bureau (2017) Agriculture facts, <http://www.arfb.com/pages/education/ag-facts/>. Accessed 22 November 2017.
- Arkansas State University (2016) The Arkansas State University system 2015-2016 factbook, Office of Institutional Research and Planning. 1-91.
- Amemiya T (1985) *Advanced Economics*. Harvard University Press, Massachusetts.
- Belsley DA, Kuh E, Welsch RE (1980) *Regression diagnostics: Identifying influential data and sources of collinearity*. Wiley, New York.
- Belsley DA (1984) Demeaning conditioning diagnostics through centering. *Am. Stat.* 38:73–82, doi:10.1080/00031305.1984.10483169.
- Bosart LF, Seimon A, LaPenta KD, Dickinson MJ (2006) Supercell tornadogenesis over complex terrain: The Great Barrington, Massachusetts, Tornado on 29 May 1995. *Wea. Forecasting*, 21:897–922.
- Bradford M (1999) Historical roots of modern tornado forecasts and warnings. *Wea. Forecasting*, 14:484–491. doi:10.1175/1520-0434(1999)014<0484:HRDMTF>2.0.CO;2.
- Bradford M (2001) *Scanning the Skies: A History of Tornado Forecasting*. University of Oklahoma Press, pp 220.

- Breusch TS, Pagan AR (1979) A simple test for heteroscedasticity and random coefficient variation. *Econometrica* 47:1287–1294, doi:10.2307/1911963.
- Brewer CA, Pickle L (2002) Evaluation of methods for classifying epidemiological data on choropleth maps in series. *Ann. Assoc. Am. Geog.* 92:662–81.
- Burnham KP, Anderson DR (2002) *Model selection and multimodel inference: A practical information-theoretic approach* (2nd ed.). Springer-Verlag, New York.
- Coleman TA, Knupp KR, Spann J, Elliott JB, Peters BE (2011) The History (and Future) of tornado warning dissemination in the United States. *Am. Meteor. Soc.* 567-582. doi:10.1175/2010BAMS3062.1.
- Crichton D (1999) *The Risk Triangle, Natural Disaster Management*. Ingleton, J., (ed), Tudor Rose London.
- Cromley RG (1996) A comparison of optimal classification strategies for choroplethic displays of spatially aggregated data. *Inter. J. Geog. Infor. Sci.* 10(4): 405–24, doi:10.1080/02693799608902087.
- Edwards R (2017) The online tornado FAQ: Frequently asked questions about tornadoes. National Oceanic and Atmospheric Administration Storm Prevention Center. www.spc.ncep.noaa.gov/faq/tornado. Accessed 27 October 2017.
- ESRI (2016) ArcGIS10.4.1 desktop help. <http://resources.arcgis.com/en/help/>. Accessed 15 June 2017.
- FEMA (2002) Community wind shelters: background and research. <http://www.fema.gov/plan/prevent/bestpractices/casestudies.shtm>. Accessed 12 October 2017.
- FEMA (2008) Arkansas' tornado shelter initiative for residences and schools: Mitigation Case Studies.
- Forbes GS, Pearce ML, Dunham TE, Grumm RH (1998) Downbursts and gustnadoes from mini-bow echoes and affiliated mesoscale cyclones over central Pennsylvania. Preprints, 16th Conf. on Weather Analysis and Forecasting, Phoenix, AZ, *Amer. Meteor. Soc.*, 295–297.
- Forbes GS, Bluestein HB (2001) Tornadoes, tornadic thunderstorms, and photogrammetry: A review of the contributions by T. T. Fujita. *Bull. Amer. Meteor. Soc.* 82(1):73-96. doi:10.1175/1520-0477.
- Fortune (2017) *The global 500: The world's largest companies*, Time, New York City.
- Frame J, Markowski P (2006) The interaction of simulated squall lines with idealized mountain ridges. *Mon. Wea. Rev.*, 134(7):1919–1941, doi:10.1175/MWR3157.1
- Fujita TT (1971) Proposed characterization of tornadoes and hurricanes by area and intensity. SMRP Research Paper 91, University of Chicago, 42 pp.
- Fujita TT (1989) The Teton-Yellowstone tornado of 21 July 1987. *Mon. Wea. Rev.*, 117(9):1913–1940, doi:10.1175/1520-0493(1989)117<1913:TTYTOJ>2.0.CO;2.

- Gaffin DM (2012) The influence of terrain during the 27 April 2011 super tornado outbreak and 5 July 2012 derecho around the Great Smoky Mountains National Park. Preprints, 26th Conference on Severe Local Storms, Nashville, TN, Amer. Meteor. Soc.
- Galway JG (1985) J.P. Finley: The first severe storms forecaster. *Bull. Amer. Meteor. Soc.*, 66:1389–1395, doi:10.1175/1520-0477(1985)066<1389:JFTFSS>2.0.CO;2.
- Gosset WS (1908) The probable error of a mean. *Biometrika*, 6(1):1-25.
- Jarque CM, Bera AK (1980) Efficient tests for normality, homoscedasticity and serial Independence of regression residuals. *Economics Letters* 6(3):255–259, doi:10.1016/0165-1765(80)90024-5
- Jarque CM, Bera AK (1981) Efficient tests for normality, homoscedasticity and serial independence of regression residuals: Monte Carlo evidence. *Econ. Let.* 7(4):313–318, doi:10.1016/0165-1765(81)90035-5.
- Jarque CM, Bera AK (1987) A test for normality of observations and regression residuals. *Inter. Stat. Rev.* 55(2):163–172.
- Karstens CD, Gallus WA, Lee BD, Finley CA (2013) Analysis of tornado-induced tree fall using aerial photography from the Joplin, Missouri, and Tuscaloosa–Birmingham, Alabama, tornadoes of 2011. *J. Appl. Meteor. Climatol.*, 52:1049–1068, doi:10.1175/JAMC-D_12_0206.1.
- Kellner O, Niyogi D (2013) Land-surface heterogeneity signature in tornado climatology: An illustrative analysis over Indiana 1950-2012. *Earth Inter.*, 18(10):1-32, doi:10.1175/2013EI000548.1.
- Koenker R (1981) A Note on studentizing a test for heteroscedasticity. *J. Econometrics* 17(1):107–112, doi:10.1016/0304-4076(81)90062-2.
- Konishi S, Kitagawa G (2008) *Information Criteria and Statistical Modeling*, Springer, New York.
- Kuligowski ED, Lombardo FT, Phan LT, Levitan ML, Jorgensen DP (2014) Final report, National Institute of Standards and Technology (NIST) technical investigation of the May 22, 2011, tornado in Joplin, Missouri. *Nat. Const. Safety Team Act Rep, NIST NCSTAR 3:1-428*, doi:10.6028/NIST.NCSTAR.3.
- LaPenta KD, Bosart LF, Galarneau TJ, Dickinson MJ (2005) A multiscale examination of the 31 May 1998 Mechanicville, New York, Tornado, *Weather and Forecasting, Am. Meteor. Soc.* 20(1):494-516, doi:10.1175/WAD875.1.
- Lewellen DC (2012) Effects of topography on tornado dynamics: a simulation study. 26th Conference on Severe Local Storms (5 - 8 November 2012) Nashville, TN, Am. Meteor. Soc. <https://ams.confex.com/ams/26SLS/webprogram/Paper211460.html>. Accessed 6 November 2017.
- Lyza AW, Knupp KR (2013) An observational analysis of potential terrain influences on tornado behavior. Severe Weather Institute and Radar & Lightning Laboratories (SWIRLL), University of Alabama, Huntsville. Internal Paper. 1-7.

- Markowski PM, Dotzek N (2011) A numerical study of the effects of orography on supercells. *J. Atmos. Res.*, 100:457-478, doi:10.1016/j.atmosres.2010.12.027.
- National Climatic Data Center (2013) U.S. tornado climatology. <http://www.ncdc.noaa.gov/oa/climate/severeweather/tornadoes.html>. Accessed 22 November 2017.
- NOAA (2017) Converting traditional hail size descriptions, Storm Prediction Center, <http://www.spc.noaa.gov/misc/tables/hailsizes.htm>, Accessed 22 November 22, 2017.
- NOAA (2017) SPC tornado, hail, and wind database format specification (for .csv output). <http://www.spc.noaa.gov/wcm/#data>. Accessed 15 September 2017.
- O'Brien RM (2007) A caution in regarding rules of thumb for variance inflation factors. *Quality & Quantity* 41:673-690, doi:10.1007/s11135-006-9018-6
- Safeguard (2009) Safeguard storm shelters - Fujita Scale. <http://www.safeguardshelters.com/fujitascale.php>. Accessed 21 October 2017.
- Selvam RP, Ahmed NS, Yousof MA, Strasser M, Ragan Q (2014) Study of Tornado Terrain Interaction from Damage Documentation of April 27, 2014 Mayflower, AR Tornado. Department of Civil Engineering, University of Arkansas, Fayetteville, AR 72701.
- Selvam RP, Ahmed NS, Yousof MA, Strasser M, Costa A (2015) RAPID: Documentation of tornado track of mayflower tornado in hilly terrain.
- Sun M, Wong DW, Kronenfeld BJ (2015) A classification method for choropleth maps incorporating data reliability information, *Prof. Geog.*, 67(1):72-83, doi:10.1080/00330124.2014.888627.
- Steel RDG, Torrie, JH (1960) *Principles and Procedures of Statistics with Special Reference to the Biological Sciences*. McGraw Hill.
- Tobler W (1970) A computer movie simulating urban growth in the Detroit region. *Econ. Geogr.* 46:234-240. doi:10.2307/143141.
- United States Census Bureau (2016) Annual estimates of the resident population: April 1, 2010 to July 1, 2016, U.S. Census Bureau Population Division, <https://factfinder.census.gov>. Accessed 22 November 2017.
- University of Arkansas (2017) Fall 2017 11th day enrollment report, Office of Institutional Research and Assessment, <https://oir.uark.edu/students/enrollment-report.php>, Accessed 22 November 2017.
- Xiao N, Calder CA, Armstrong MP (2007) Assessing the effect of attribute uncertainty on the robustness of choropleth map classification. *Int. J. Geog. Inf. Sci.* 21 (2):121-44, doi:0.1080/13658810600894307.

CHAPTER 4

CONCLUSION

The main objective of this research could be summed up as to whether or not GIS could be used to affectively address spatio-temporal patterns associated with major geohazards. Much focus has been conducted on earthquakes because of the pandemonium and obsession with the New Madrid Earthquake of 1812 and the Guy-Quitman Swarm 2010-2011 associated with a compromised injection well. Apart from these focal points, detailed research on severe geohazards had been tragically understudied in Arkansas and offering some remedy to that deficiency was the foremost aim of this research. Much headway was gained through this research by using ArcGIS to unlock, model, and statistically analyze the patterns in each respective dataset allowing high confidence prediction of susceptibility and severity.

Speaking for the mass wasting research, possibly one of the biggest contributions was bringing attention to detail during data collection and dataset creation for the landslide team at ArDOT. Lack of critical information, especially temporal information associated with locations of failures along highways is a critical next step in doing high quality landslide susceptibility work. It was not apparent before this study that ArDOT include these ancillary attributes in their data catalogs. This problem has been remedied for the future which opens a whole new field of research that can be conducted on down the road.

The mass-wasting susceptibility modeling used a novel and very effective approach to model and predict future areas of high risk by sifting and weighting inputs with the Analytical Hierarchy Process (AHP) and then going for an Occam's Razor approach of just using the very most significant variables for modeling and then applying a hybridization of Fuzzy modeling and Empirical Bayesian Kriging to generate the final susceptibility model. Roads were entirely

removed from the model to minimize any bias, and the best attempts were made to reduce a priori weighted bias to the datasets by applying the AHP. The model was verified against the observed road failures by ArDOT, which constituted, by far, the largest collection of mass wasting events in Arkansas but only was focused around major roadways and neglected essentially the rest of all non-paved roadways and land. This novel approach achieved an approximately 83% accuracy, while a heavily biased Weighted Overlay (WO) approach, modeled susceptibility using all significant explanatory variables. This WO approach was wrought with multi-collinearity biased issues and heavily focused on roads as the root cause behind these failures only managed to predict ~28% of failures.

Quality scientific research and attention to detail allowed this mass wasting research to be published in Springer's Journal of Natural Hazards as Rowden KW, Aly MH (2018) A novel triggerless approach for mass wasting susceptibility modeling applied to the Boston Mountains of Arkansas, USA, *Natural Hazards*, pp 1–21, doi:10.1007/s11069-018-3201-7. This should speak volumes for itself and now this research can be queried and accessed all over the world. With time, techniques from this novel approach will hopefully be implemented by other researchers across the globe and add provide solutions to regions analogous to the Boston Mountains.

The second part of this research also employed GIS to address spatial patterns within complex severe weather data. The National Oceanic and Atmospheric Agency (NOAA) and their syndicates of the National Weather Service (NWS) and Storm Prediction Center (SPC) catalog and broadly analyze severe weather across the United States but little outside of individual storm systems is worked with. Within the state level Arkansas Department of Emergency Management (ADEM) and the local branches of the NWS choose to look at severe weather risk at the county level or as hotspot on kernel density heat maps. Both of these common approaches put Arkansans

at a great disadvantage of knowing their state of vulnerability at their location of residence. What this research successfully did was systematically fishnet the state in 10x10km grids and then assign severe weather events to each grid, building a sizeable attribute catalog of potential explanatory variables to which Exploratory Regression and Ordinary Least Squares regression techniques were used to whittle out the most significant explanatory variables influencing the spatial patterns observed in the NWS/SPC datasets.

What these aggregate to is a unique and highly detailed analysis into weather severity at a very focused local level for the entire state. The products from this research, could (and should), be used by state entities such as FEMA and the Governor's Office to plan for better ways to inform and protect Arkansans living in the path of highest risk. Federal grants and state grants exist for subsidize storm shelters and to my astonishment during interviews with Arkansans all across the state not one single person knew there is free money out there to build a storm shelter on their property. Yet, everyone fears tornadoes and worries about where to seek shelter during a severe thunderstorm capable of generating tornadoes, derechos, and large hail.

It is my upmost hope that this part of the thesis research will be taken to heart and influence public opinion. In cases such as the April 2014 Mayflower Tornado which completely decimated a neighbor and took 16 lives, a large neighborhood shelter could have greatly changed the outcome of that tragic event. This is the quintessential essence of hazard mitigation. We research deeply into a problem and create a model that explains and accurately predicts future areas of risk so that the general public can educate themselves and plan for the worst and the governmental bodies in charge of taking the public's best interest to heart can plan larger-scale and more costly ways of mitigating risk. Knowledge is power and therefore as scientists it is so important to speak scientific truth to power, especially in cases of governmental negligence or ignorance.

As with the first paper, the quality of research and attention to scientific detail lead to this second paper being published in Springer's Journal of Geoenvironmental Disasters as: Rowden KW, Aly MH (2018) GIS-based regression modeling of the extreme weather patterns in Arkansas, USA, *Geoenvironmental Disasters*, pp 1-15, doi:10.1186/s40677-018-0098-0. This should speak volumes to the quality of research which has been peer-reviewed in an open-access international journal and hopefully lead researchers all over the world to these techniques for furthering their own research and mitigating risk in their areas of focus.

GIS is a powerful system. GIS pools from all fields of science and blends these diverse theories and algorithms in a software package that can uniquely and effectively handle complex spatial and temporal problems. GIS applications proliferate through all realms of research institutions, private sector, and public-sector agencies and institutions. Therefore, GIS was a logical vehicle for exploring spatial and temporal patterns within big datasets.

REFERENCES

- Berry, E. W., 1915, Erosion Intervals in the Eocene of the Mississippi Embayment: U. S. Geological Survey Professional Paper 95-F.
- Clardy, B. F., 1979, Arkansas Lignite Investigations, Preliminary Report: Arkansas Geological Commission Miscellaneous Publication 15.
- Cphoon RR (2013) Geologic Roadguide to the Scenic 7 Byway. Little Rock, AR
- Craig, W. W., Wise, O., and McFarland, J. D., 1984, A Guidebook to the Post-St. Peter Ordovician and the Silurian and Devonian Rocks of North-Central Arkansas: Arkansas Geological Commission Guidebook 84-1.
- Croneis, C., 1930, Geology of the Arkansas Paleozoic Area: Arkansas Geological Commission Bulletin 3.
- Dane, C. H., 1929, Upper Cretaceous Formations of Southwestern Arkansas: Arkansas Geological Commission Bulletin 1.
- Guccione, M. J., Prior, W. L., and Rutledge, E. M., 1986, The Tertiary and Quaternary Geology of Crowley's Ridge: Arkansas Geological Commission Guidebook 86-4.
- Haley, B. R., et al., 1976, 1993 (revised), Geologic Map of Arkansas: Arkansas Geological Commission.
- Harris, G. D., 1894, The Tertiary Geology of Southern Arkansas: Annual Report of the Geological Survey of Arkansas for 1892, Volume II.
- Hill, R. T., 1888, The Neozoic Geology of Southwestern Arkansas: Annual Report of the Geological Survey of Arkansas for 1888, Volume II.
- Sutherland, P. K. and Manger, W. L., 1977, Upper Chesterian-Morrowan Stratigraphy and the Mississippian-Pennsylvanian Boundary in Northeastern Oklahoma and Northwestern Arkansas: Oklahoma Geological Survey Guidebook 18.
- Sutherland, P. K. and Manger, W. L., 1979, Mississippian-Pennsylvanian Shelf-to-Basin Transition Ozark and Ouachita Regions, Oklahoma and Arkansas: Oklahoma Geological Survey Guidebook 19.